

Chapter 4

Accelerator and Muon Delivery

In order to achieve a statistical uncertainty of 0.1 ppm, the total ($g-2$) data set must contain at least 1.8×10^{11} detected positrons with energy greater than 1.8 GeV, and arrival time greater than $30 \mu\text{s}$ after injection into the storage ring. This is expected to require 4×10^{20} protons on target including commissioning time and systematic studies. For optimal detector performance, the number of protons in a single pulse to the target should be no more than 10^{12} and the number/fraction(?) of secondary protons transported into the muon storage ring should be less than ???. Data acquisition limits the time between pulses to be at least 10 ms. The revolution time of muons around the storage ring is 149 ns, and therefore the experiment requires the bunch length to be no more than ~ 100 ns. Systematic effects on muon polarization limit the momentum spread dp/p of the secondary beam. Requirements and general accelerator parameters are given in Table 4.1.

Parameter	Design Value	Requirement	Unit
Total protons on target	$2.3 \times 10^{20}/\text{year}$	4×10^{20}	protons
Interval between beam pulses	≥ 10	≥ 10	ms
Max bunch length (full width)	120 (95%)	< 149	ns
Intensity of single pulse on target	10^{12}	10^{12}	protons
Max Pulse to Pulse intensity variation	± 10	± 50	%
dp/p of pions accepted in decay line	2-5	2	%
Momentum of muon beam	3.094	3.094	GeV/c
Stored muons per 10^{12} proton on target	10^5 into inflector	≥ 6000	muons
dp/p of muons into ring	0.5	0.5	%
Fraction of beam into ring which is protons	1??	$< 10??$	%

Table 4.1: General beam requirements and design parameters.

4.1 Overall Strategy

The ($g-2$) experiment at Fermilab is designed to take advantage of the infrastructure of the former Antiproton Source, as well as improvements to the Proton Source and the

conversion of the Recycler to a proton-delivery machine. It is also designed to share as much infrastructure as possible with the Mu2e experiment in order to keep overall costs low.

The Antiproton Accumulator will no longer be in use, and many of its components will be reused for the new and redesigned Muon beamlines. Stochastic cooling components and other infrastructure no longer needed in the Debuncher ring will be removed in order to improve the aperture, proton abort functionality will be added, and the ring will be renamed the Delivery Ring (DR). The former AP1, AP2, and AP3 beamlines will be modified and renamed M1, M2, and M3. The DR Accelerator Improvement Project (AIP) will provide upgrades to the Delivery Ring as well as aperture improvements to the P1, P2, and M1 lines needed for future muon experiments using 8 GeV protons, including $(g - 2)$. The layout of the beamlines is shown in Fig. 4.1.

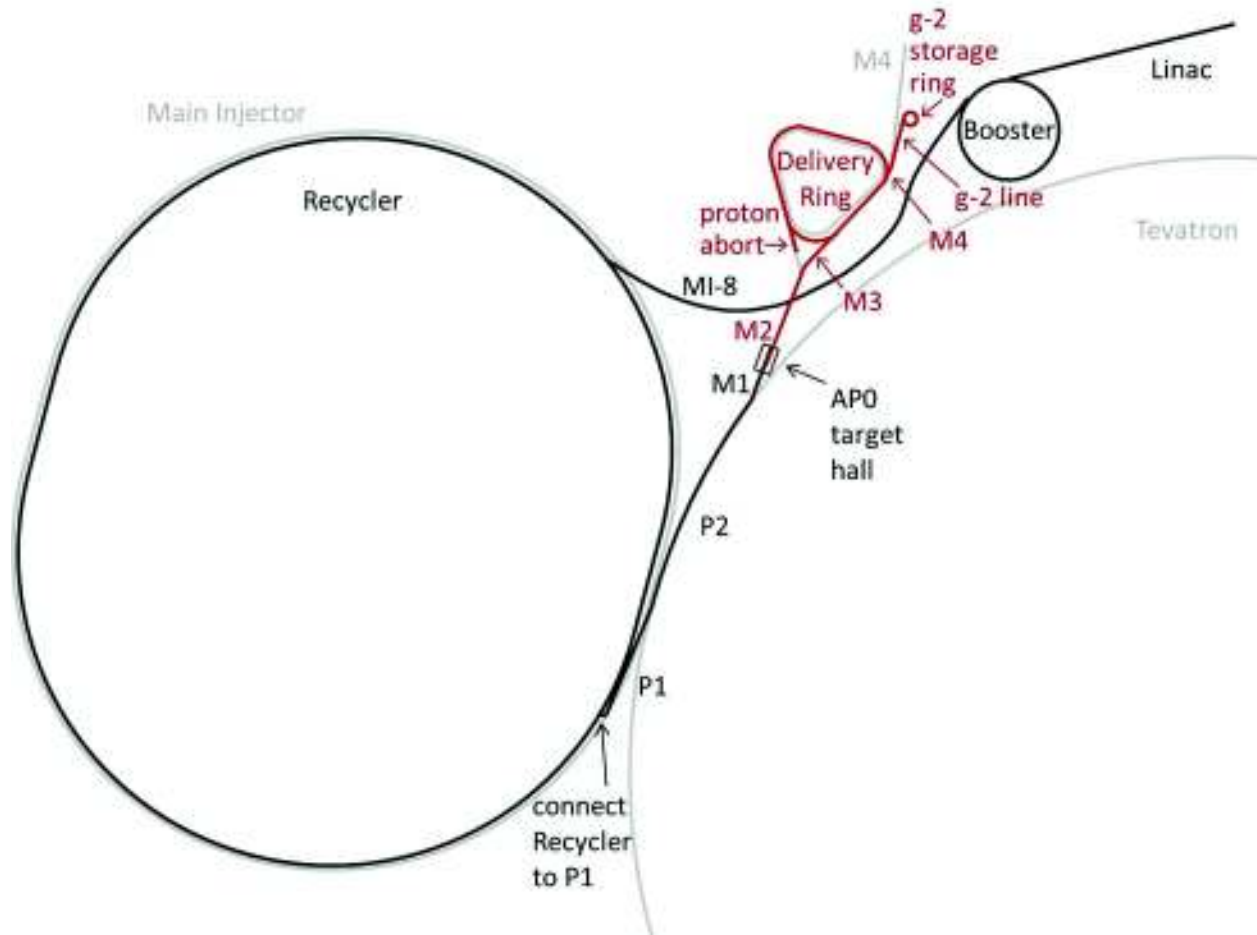


Figure 4.1: Path of the beam to $(g - 2)$. Protons (black) are accelerated in the Linac and Booster, are re-bunched in the Recycler, and then travel through the P1, P2, and M1 lines to the APO target hall. Secondary beam (red) then travels through the M2 and M3 lines, around the Delivery Ring, and then through the M4 and $(g - 2)$ lines to the muon storage ring.

The Proton Improvement Plan [1], currently underway, will allow the Booster to run at 15 Hz, at intensities of 4×10^{12} protons per Booster batch. Following the completion

of the Accelerator and NuMI Upgrades (ANU) subproject at Fermilab to prepare for the NO ν A experiment [2], the Main Injector (MI) will run with a 1.333 s cycle time for its neutrino program, with twelve batches of beam from the Booster being accumulated in the Recycler and single-turn injected into the MI at the beginning of the cycle. While the NO ν A beam is being accelerated in the MI, eight Booster batches will be available for experimental programs such as ($g - 2$) which use 8 GeV protons. The ANU subproject will also enable injection from the Booster into the Recycler. Extraction from the Recycler to the P1 beam line, required for ($g - 2$), will be implemented in the Recycler AIP.

Protons from the Booster with 8 GeV kinetic energy will be re-bunched into four smaller bunches in the Recycler and transported through the P1, P2, and M1 beamlines to a target at AP0. Secondary beam from the target will be collected using a focusing device, and positively-charged particles with a momentum of 3.11 GeV/c will be selected using a bending magnet. Secondary beam leaving the target station will travel through the M2 and M3 lines which are designed to capture as many muons with momentum 3.094 GeV/c from pion decay as possible. The beam will then be injected into the Delivery Ring. After several revolutions around the DR, essentially all of the pions will have decayed into muons, and the muons will have separated in time from the heavier protons. A fast kicker will then be used to abort the protons, and the muon beam will be extracted into the new M4 line, and finally into the new ($g - 2$) beam line which leads to the ($g - 2$) storage ring. Note that the M3 line, Delivery Ring, and M4 line are also designed to be used for 8 GeV proton transport by the Mu2e experiment.

The expected number of muons transported to the storage ring, based on target-yield simulations using the antiproton-production target and simple acceptance assumptions, is 1×10^5 ???. Beam tests were conducted using the existing Antiproton-Source configuration with total charged-particle intensities measured at various points in the beamline leading to the Debuncher, which confirmed the predicted yields to within a factor of two(???) [3]. More details are given in Sec. 4.4.1.

4.2 Protons from Booster

During the period when ($g - 2$) will take data, the Booster is expected to run with present intensities of 4×10^{12} protons per batch, and with a repetition rate of 15 Hz. In a 1.333 s Main-Injector super cycle, twelve Booster batches are slip-stacked in the Recycler and then accelerated in the MI and sent to NO ν A. While the Main Injector is ramping, a time corresponding to eight Booster cycles, the Recycler is free to send 8 GeV (kinetic energy) protons to ($g - 2$). The RF manipulations of beam for ($g - 2$) in the Recycler (Sec. 4.3.1) allow ($g - 2$) to take every-other of the eight available Booster batches. Figure 4.2 shows the time structure of beam pulses to ($g - 2$).

The following section describes improvements needed to run the proton source reliably at 15 Hz.

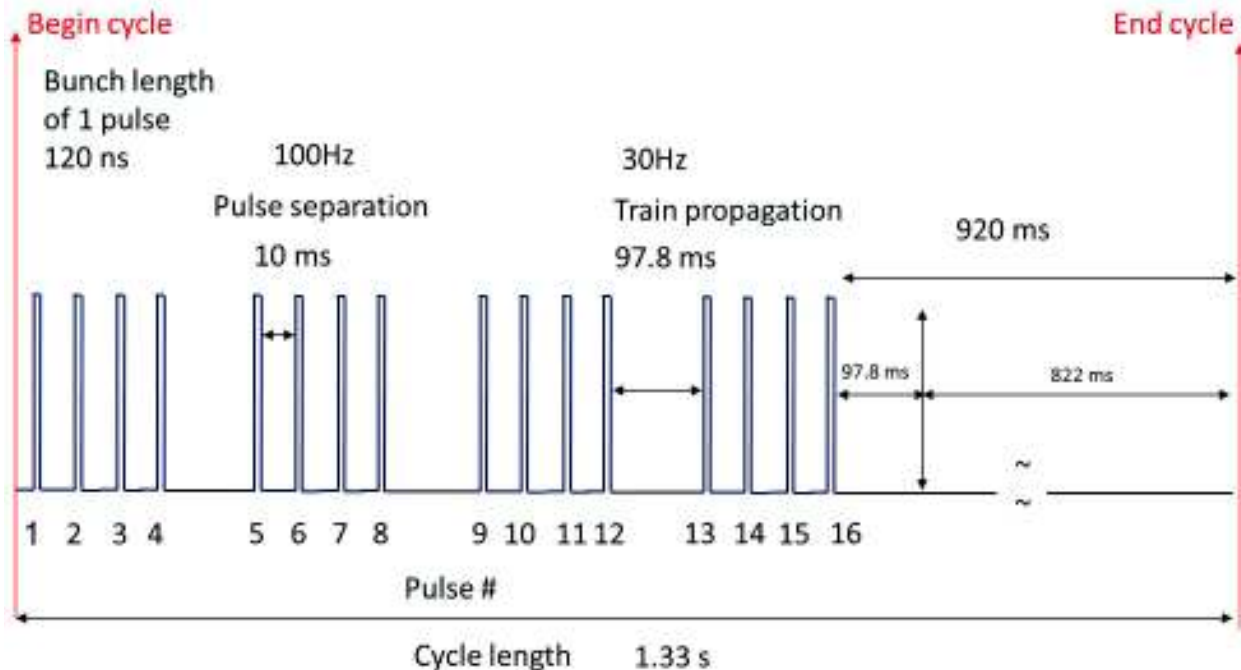


Figure 4.2: Time structure of beam pulses to $(g - 2)$.

4.2.1 Proton Improvement Plan

The Fermilab Accelerator Division has undertaken a Proton Improvement Plan (PIP) [1] with the goals of maintaining viable and reliable operation of the Linac and Booster through 2025, increasing the Booster RF pulse repetition rate, and doubling the proton flux without increasing residual activation levels.

The replacement of the Cockroft-Walton pre-accelerator with an RFQ during the 2012 shutdown is expected to increase reliability of the pre-accelerator and to improve beam quality.

The Booster RF solid-state upgrade is necessary for reliable 15 Hz RF operations. This involves the replacement of 40-year-old electronics that are either obsolete, difficult to find, or unable to run at the required higher cycle-rate of 15 Hz, and will allow for easier maintenance, shorter repair times, and less radiation exposure to personnel. The solid-state upgrade will be completed in 2013.

Refurbishment of the Booster RF cavities and tuners, in particular, cooling, is also necessary in order to operate at a repetition rate of 15 Hz.

Other upgrades, replacements, and infrastructure improvements are needed for viable and reliable operation. Efforts to reduce beam loss and thereby lower radiation activation include improved methods for existing processes, and beam studies, e.g., aimed at finding and correcting aperture restrictions due to misalignment of components.

The proton flux through the Booster over the past two decades and projected into 2016 based on expected PIP improvements is shown in Fig. 4.3.

The new PIP flux goal will double recent achievements and needs to be completed within five years. Figure 4.4 shows both the increase in flux as well as planned users. The goal

of doubling the proton flux will be achieved by increasing the number of cycles with beam. The intensity per cycle is not planned to increase.

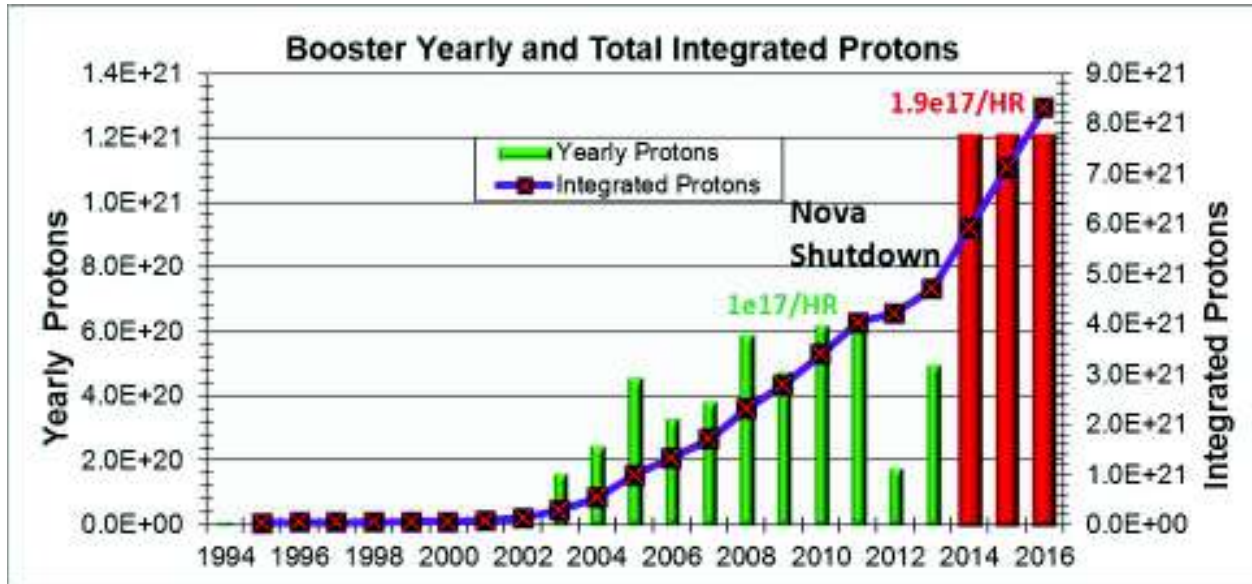


Figure 4.3: Yearly and integrated proton flux (including PIP planned flux increase).

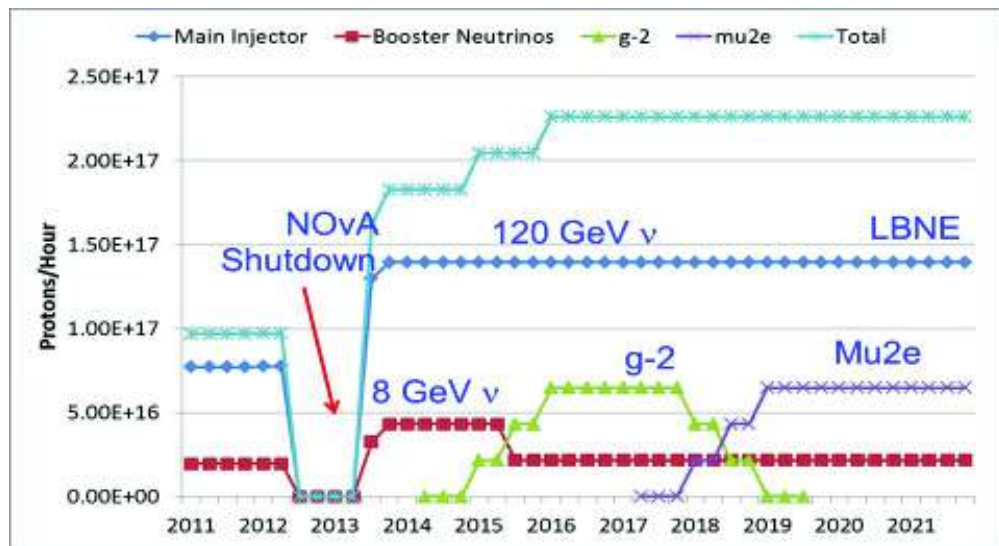


Figure 4.4: Expectations for increases in the proton flux from the Proton Source needed for future experiments.

4.3 Recycler

The $(g - 2)$ experiment requires a low number of decay positrons in a given segment of the detector, and therefore requires that the full-intensity (4×10^{12} protons) bunches be redistributed into four bunches of 1×10^{12} protons. These bunches should be spaced no closer than 10 ns to allow for muon decay and data acquisition in the detector. Because the revolution time of muons in the $(g - 2)$ ring is 149 ns, and the time needed for the ring kicker to fire is XX, the longitudinal extent of the bunches should be no more than 120 ns. The Recycler modifications needed to achieve these requirements will be made under the Recycler AIP, and are described below.

4.3.1 Recycler RF

The proposed scheme for $(g - 2)$ bunch formation [4] uses one RF system, 80 kV of 2.5 MHz RF. The design of the RF cavities will be based on that of existing 2.5 MHz cavities which were used in collider running, but utilizing active ferrite cooling. The ferrites of the old cavities and the old power amplifiers will be reused in the new system.

In order to avoid bunch rotations in a mismatched bucket, the 2.5 MHz is ramped “adiabatically” from 3 to 80 kV in 90 ms. Initially the bunches are injected from the Booster into matched 53 MHz buckets (80 kV of 53 MHz RF), then the 53 MHz voltage is turned off and the 2.5 MHz is turned on at 3 kV and then ramped to 80 kV. The first 2.5 MHz bunch is then extracted and the remaining three bunches are extracted sequentially in 10 ms intervals. The formation and extraction of all four bunches takes two Booster ticks or 133 ms. This limits the $(g - 2)$ experiment to using four of the available eight Booster ticks in every Main-Injector super cycle.

Simulated 2.5 MHz bunch profiles are shown in Fig. 4.5. The 53 MHz voltage was ramped down from 80 to 0 kV in 10 ms and then turned off. The 2.5 MHz voltage was snapped to 3 kV and then adiabatically raised to 80 kV in 90 ms. The overall efficiency is 95%, and 95% of the beam captured is contained within 120 ns. The maximum momentum spread is $dp/p = \pm 0.28\%$.

Although the Recycler is not yet configured to do such RF manipulations, by using the 2.5 MHz coalescing cavities in the Main Injector, the proposed bunch-formation scheme was tested with beam. In general, the agreement between simulations and data is very good. For illustration, the comparison between the beam measurements and the simulations for the case in which the 2.5 MHz voltage is ramped adiabatically from 3 to 70 kV in 90 ms is shown in Fig. 4.6.

Extraction from the Recycler and primary proton beam transport will be described in the beamline section, Sec. 4.5.

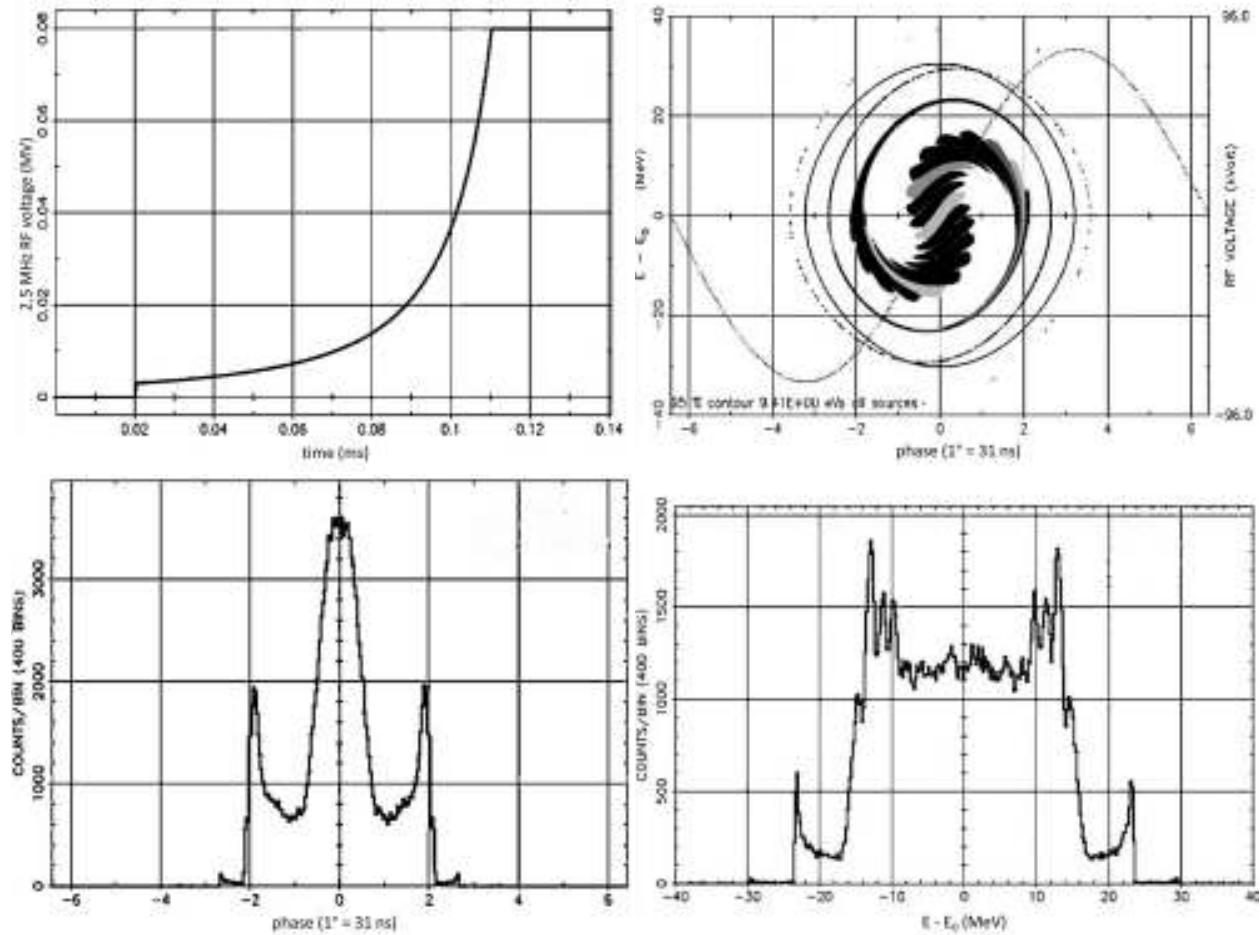


Figure 4.5: Results of RF simulations: 2.5 MHz voltage curve (upper left), phase space distribution (upper right), phase projection (lower left) and momentum projection (lower right).

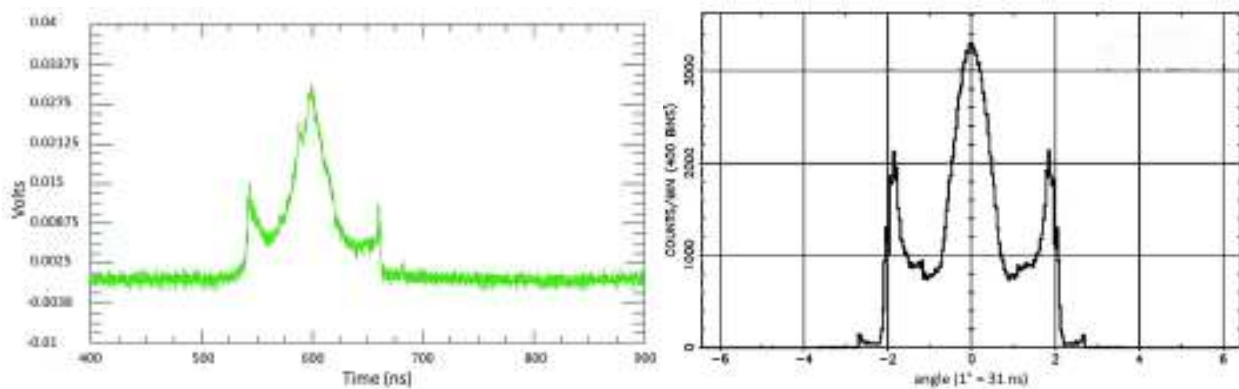


Figure 4.6: Comparison of beam profile (left) with simulation (right) for the case in which the 2.5 MHz voltage is ramped “adiabatically” from 3-70 kV in 90 ms. In both profiles, 95% of the particles captured are contained within 120 ns.

4.4 Target station

The $(g - 2)$ production target station will reuse the existing target station that has been in operation for antiproton production for the Tevatron Collider for 23 years, while incorporating certain modifications. The $(g - 2)$ target station will be optimized for maximum π^+ production per proton on target (POT) since the experiment will utilize muons from pion decay. Repurposing the antiproton target station to a pion production target station takes full advantage of a preexisting tunnel enclosure and service building with no need for civil construction. Also included are target vault water cooling and air ventilation systems, target systems controls, remote handling features with sound working procedures and a module test area. Figure 4.7 shows the current target-station (vault) layout. The overall layout of the target-vault modules will be unchanged from that used for antiproton production. The major differences in design will include different primary and secondary beam energies, polarity of the selected particles and pulse rate. Upgrades to pulsed power supplies, target design, pulsed-magnet design and the target dump are all considered.

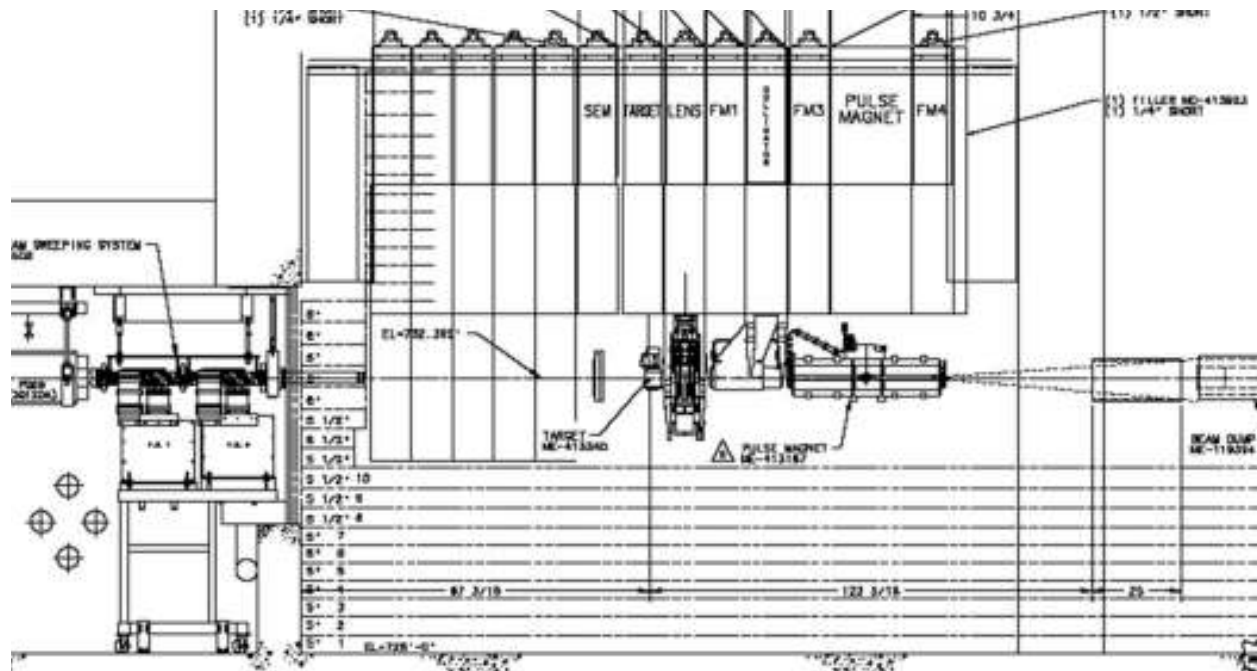


Figure 4.7: Layout of the $(g - 2)$ target station.

The production target station consists of five main devices: the pion production target, the lithium lens, a collimator, a pulsed magnet, and a beam dump. Once the primary beam impinges on the target, secondaries from the proton-target interaction are focused by the lithium lens and then momentum-selected, centered around a momentum of 3.094 GeV/c, by a pulsed dipole magnet (PMAG). This momentum is the magic momentum needed to measure the muon anomalous magnetic moment in the downstream muon ring. The momentum-selected particles are bent 3° into a channel that begins the M2 beam line. Particles that are not momentum-selected will continue forward and are absorbed into the target-vault dump. An overview of some of the required beam design parameters for the $(g - 2)$ target system

can be found in Table 4.2.

Parameter	FNAL ($g - 2$) 12 Hz
Intensity per pulse	10^{12} p
Total POT per cycle	16×10^{12} p
Number of pulses per cycle	16
Cycle length	1.33 s
Primary energy	8.89 GeV
Secondary energy	3.1 GeV
π^+ production / POT	0.9×10^{-5}
p production / POT	2.0×10^{-5}
μ^+ production / POT	0.007×10^{-5}
Beam power at target	17.2 kW
Beam size σ at target	0.15 mm
Selected particle	π^+
dp/p (PMAG selection)	5%

Table 4.2: Beam parameters for the target station.

One significant difference the ($g - 2$) production target station will have from the antiproton production target station is the pulse rate at which beam will be delivered to the target station. The ($g - 2$) production rate will need to accommodate 16 pulses in 1.33 s with a beam pulse-width of 120 ns. This is an average pulse rate of 12 Hz. The antiproton production pulse rate routinely operated at 1 pulse in 2.2 s or 0.45 Hz. This will be a challenging factor that can drive the cost of the design since the lithium lens and pulsed magnet will need to pulse at a significantly higher rate. Figure 4.2 shows the ($g - 2$) pulse scenario for pulsed devices and timing for proton beam impinging on the target.

4.4.1 The ($g - 2$) production target and optimization of production

The current default target to be used for the ($g - 2$) experiment is the antiproton production target used at the end of the Tevatron Collider Run II. This target should be able to produce a suitable yield of approximately 1.0×10^{-5} π^+ /POT. This target design has a long history of improvements for optimization and performance during the collider run. The target is constructed of a solid Inconel 600 core and has a radius of 5.715 cm with a typical chord length of 8.37 cm. The center of the target is bored out to allow for pressurized air to pass from top to bottom of the target to provide internal cooling to the Inconel core. It also has a cylindrical beryllium outer cover to keep Inconel from being sputtered onto the lithium lens from the impinging protons. The target has a motion control system that provides three-dimensional positioning with rotational motion capable of 1 turn in 45 s. This target and the target motion system need no modifications or enhancements to run for the ($g - 2$) experiment. Figure 4.8 shows a drawing and a photo of the current target.

Summarize results of beam tests and comparison to simulation.

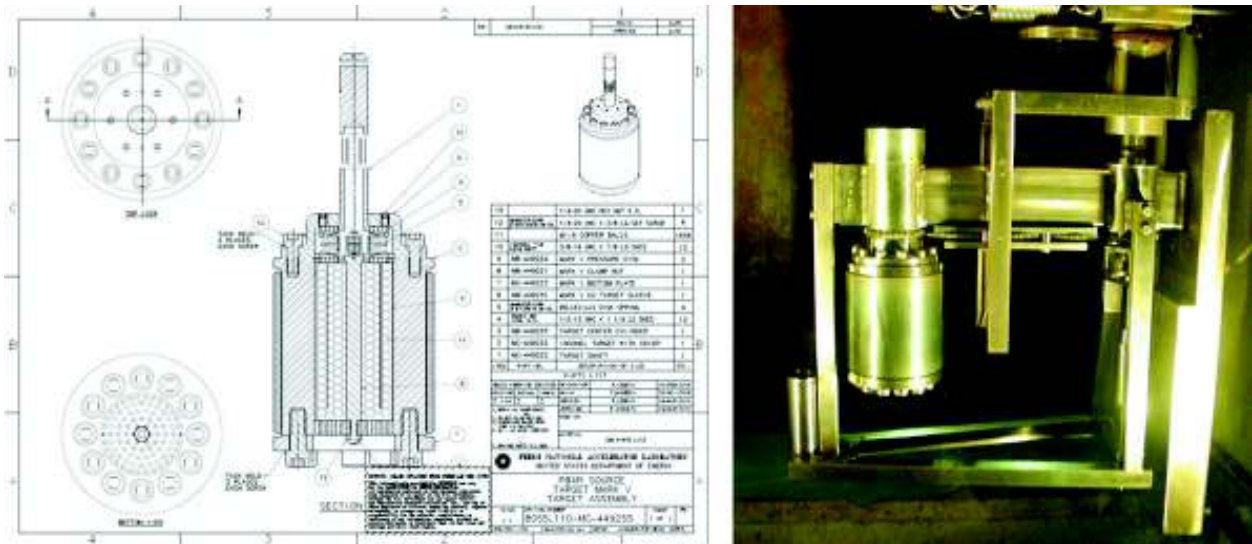


Figure 4.8: Current default target to be used for the $(g - 2)$ target station.

Even though this target is expected to produce a reasonable yield of about $10^{-5} \pi^+/\text{POT}$ for the $(g - 2)$ experiment, significant effort has been put into investigating a cost-effective, practical target design that will be optimized for pion production. Simulations have been conducted using MARS [6] to determine the optimal parameters, including impinging proton spot size at the target, target material, target length and thickness, and target orientation [7]. A graphical representation of the target system as implemented in the MARS15 code is shown in Fig. 4.9.

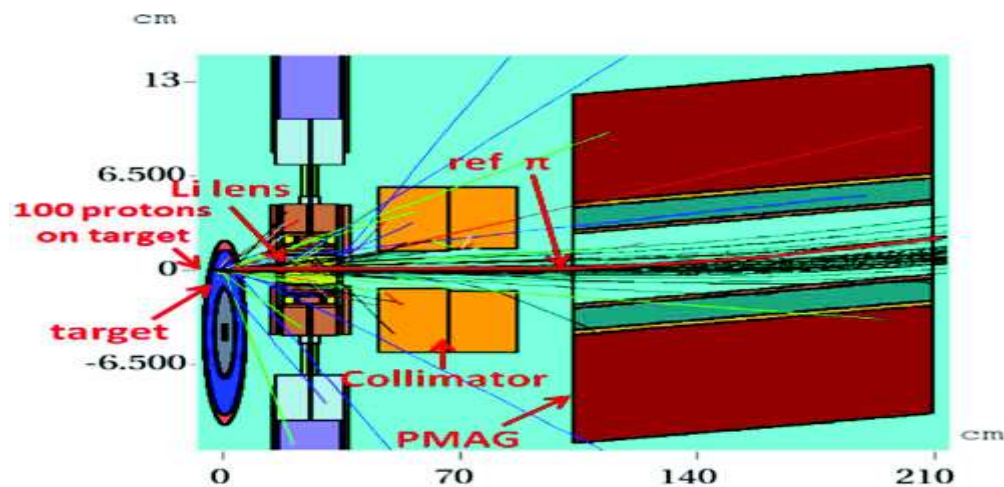


Figure 4.9: Graphical representation of target system used in MARS for simulated yield results.

The spot size of the beam on the target is an important parameter in determining the pion yield. Initial values for the spot size were simply scaled from the $\sigma_x = \sigma_y = 0.15$ mm size of the beam for 120 GeV antiproton production to $\sigma_x = \sigma_y = 0.55$ mm for 8.9 GeV. Optimized results from the MARS simulations for the impinging-proton spot size can be seen

in Fig. 4.10. This plot shows the dependence of pion yield per POT on the beta function β at half distance into the target for the current default target. A reasonable range of expected β 's which can be achieved is from 2.5 to 3.5 cm. The simulation result demonstrates that if the spot size is reduced from the original 0.55 mm to 0.15 mm, a 40-60% increase in pion production can be achieved [8] depending on β . These modifications are not directly made to the target station or target components but to the beam line just upstream of the target. Details of the beam line optics incorporating this optimization for pion yield can be found in Sec 4.5.4.

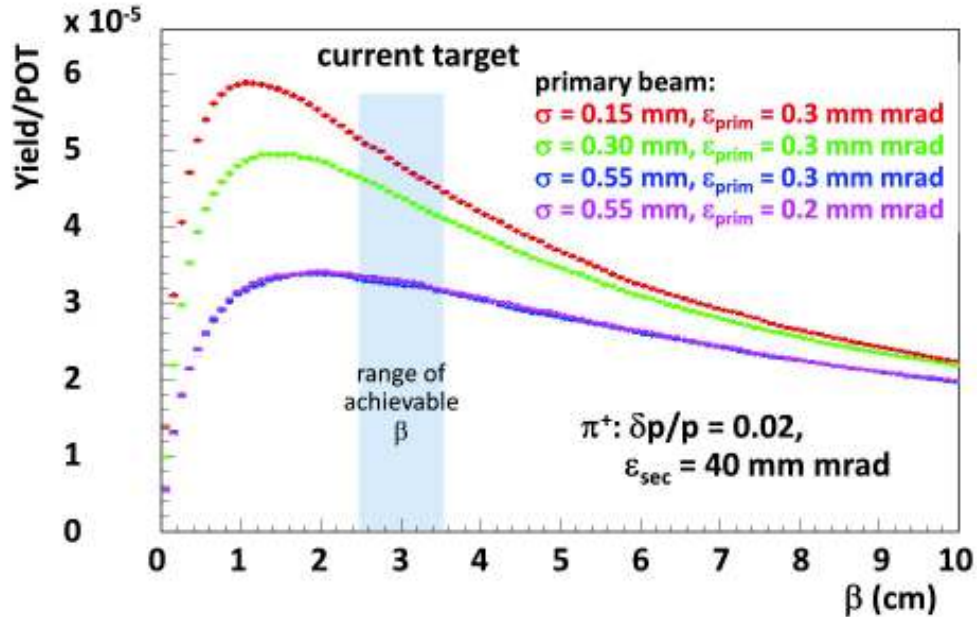


Figure 4.10: MARS simulation result for dependence of pion yield on β for different target spot sizes for a proton beam of emittance ϵ_{prim} and secondary beam momentum spread $dp/p = 0.02$ and emittance $\epsilon_{sec} = 40$ mm mrad.

Also, optimizations concerning parameters for the target material, target length, and target width were also considered. First considered were optimizations to the target material. Three materials were simulated: Inconel, tantalum and carbon. Figure 4.11 illustrates the dependence of yield vs. β at the target for different materials with optimized lengths. Inconel and carbon are shown to have higher yields than tantalum. These results, combined with Fermilab's long history of building antiproton targets with Inconel, make Inconel the favored target material.

Next considering the dimensions of the target, Fig. 4.12a illustrates that a longer target will produce higher yields, while Fig. 4.12b demonstrates a weak dependence on the target thickness or radius. Therefore, the optimal pion production target may be a cylindrical rod with a length of 89 mm and a radius of 0.6 mm. However, to favor a more practical target design that will be able to be incorporated into the existing target mechanical and cooling systems, horizontal slabs made of Inconel of various heights were simulated. The output of the MARS simulation was then placed into G4beamline [9] in order to propagate particles

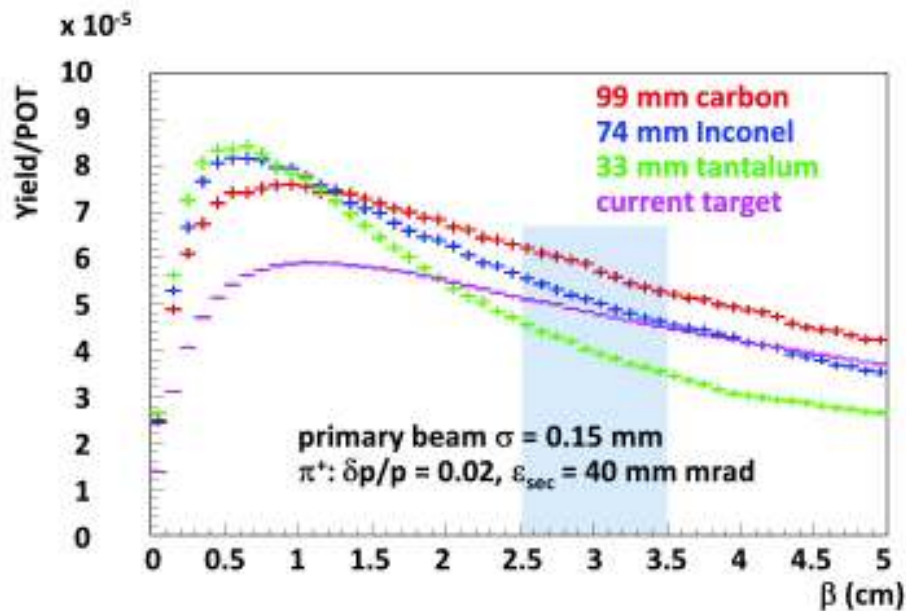


Figure 4.11: MARS simulation result for dependence of pion yield on β for different target materials. The length of the target is proportional to the interaction length of the material.

through the first four quadrupoles in the M2 beam line. Particle yields were tallied at the end of these quadrupoles with appropriate acceptance cuts for the elements. Figure 4.13 shows the pion yield for two optimized horizontal slab targets one of height 0.60 mm and the second of 0.75 mm. They are both approximately 107 mm long. Simulations for these slab targets show that a 22% and 14% gain in pion yield from optimized horizontal slabs can be obtained, respectively. Therefore, by combining the 40-60% increase from the reducing the target spot size and a 14 to 22% increase from an optimized target, a total increase of a factor of almost two in pion production may be achievable. This would be an estimated production rate of $2.0 \times 10^{-5} \pi^+/\text{POT}$ with all the suggested improvements.

The actual details for the design of the alternate target are currently being worked out. However, it is preferred that the simulated horizontal slabs transition into target discs that could be mounted on a stacked-disc style target incorporating the simulated dimensions. In order to provide cooling to the target material, the target discs would be separated by discs of low Z material like beryllium or aluminum. Figure 4.14 is a picture of a proposed design of a target incorporating stacked target and cooling discs. The blue material represents discs of Inconel separated by the grey shaded areas which would be beryllium. One consideration for operating with the stacked discs that are very thin, approximately 0.6 mm, is the need for beam stability on the target. This may require improvements in upstream trim power supplies to achieve appropriate stability. There will be beam tests in 2013 in which a prototype stacked-disc target will be constructed and tested to narrow and confirm the design of the alternate target.

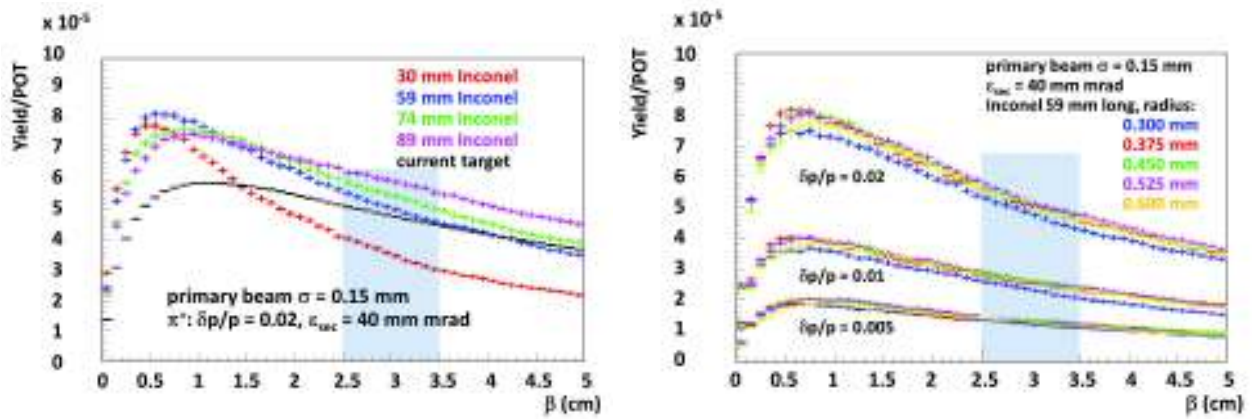


Figure 4.12: MARS simulation result for dependence of pion yield on β for different target lengths (a) and thicknesses (b).

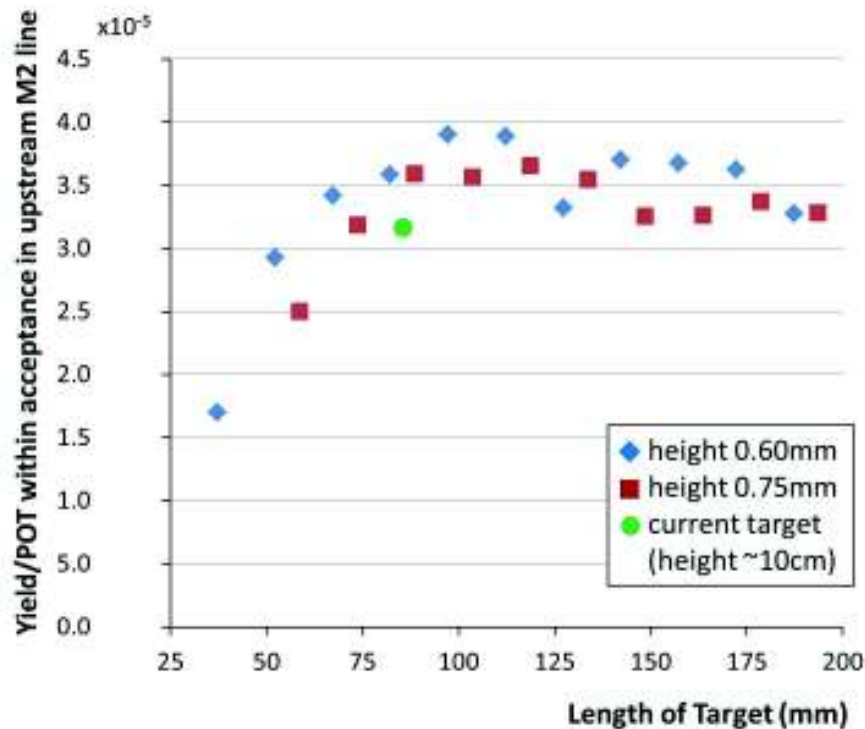


Figure 4.13: MARS/G4beamline predictions for number of pion secondaries from an Inconel target making it to the upstream M2 line as a function of target slab length for a slab of height 0.60 mm (with the upstream end of the target 56 mm from the lens focal point), a slab of height 0.75 mm (with the upstream end of the target 67 mm from the lens focal point), and the current target (assuming a chord length of 75 mm). The location of the target for a given height slab was optimized to give maximum yield. The spot size of beam on the target is taken to be 15 mm and the acceptance 40 mm mrad. A thin target of length 107 mm is predicted to give an increase in yield of 14-22% over the existing target.

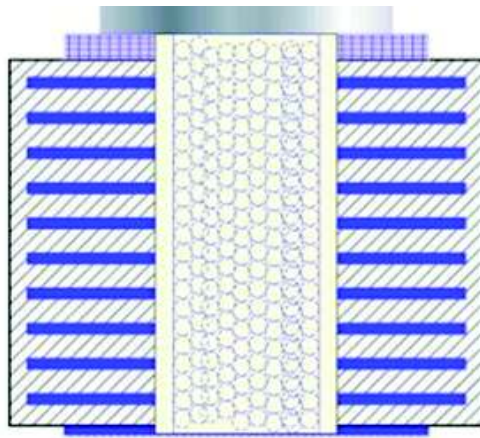


Figure 4.14: Proposal for new $(g - 2)$ target design utilizing stacked thin slabs of Inconel (blue) separated by Beryllium (hashed grey). Target material air cooling channels are in the middle of the target.

4.4.2 Focusing of secondaries from the target

The lithium collection lens is a 1 cm radius cylinder of lithium that is 15 cm long and carries a large current pulse that provides a strong isotropically focusing effect to divergent incoming secondaries after the initial interaction of impinging particles with the target [10]. The lithium lens cylinder is contained within a toroidal transformer, and both lens and transformer are water cooled. Figure 4.15 is a drawing of the lithium lens depicting (a) the transformer and lens body, and (b) details of the lithium cylinder.

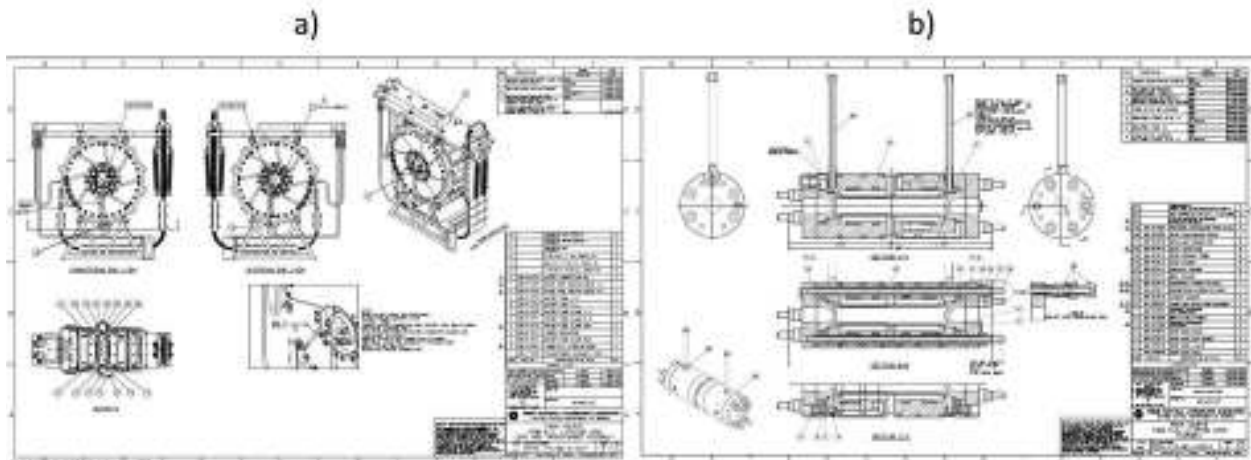


Figure 4.15: Drawing of the lithium lens and transformer (a) and the lithium cylinder body (b).

During antiproton production for the Collider Run II, the lens pulsed at a peak current of 62 kA, which is equivalent to a gradient of 670 T/m at 8.9 GeV/c with a base pulse width of 400 μ s. Scaling the lens gradient for use at 3.115 GeV/c for $(g - 2)$ and in order to accommodate a similar range of focal lengths from the target to the lens of roughly 28 cm, the gradient required will be 230 T/m at a pulsed peak current of 22 kA with the same 400 μ s pulse width. Table 4.3 provides an overview of required operating parameters. Accommodating the $(g - 2)$ 12 Hz average pulse rate for the lithium lens is one of the biggest challenges and concerns for repurposing the antiproton target station for $(g - 2)$. Even though peak current and gradient will be reduced by a factor of about 3, the pulse rate will increase by a factor of 24 compared to the operation for antiproton production. Resistive and beam heating loads, cooling capacity, and mechanical fatigue are all concerns that are warranted for running the lithium lens at the $(g - 2)$ repetition rate.

Lens operation	Pulse width (μ s)	Peak current (kA)	Gradient (T/m)	Pulses per day
Antiproton production	400	62.0	670	38,880
$(g - 2)$ pion production	400	22.6	230	1,036,800

Table 4.3: Lithium lens operation parameters.

Therefore, in order to gain confidence that the lens will be able to run under these conditions, a preliminary ANSYS [11] analysis has been conducted. This analysis simulated

thermal and mechanical fatigue for the lens based on the pulse timing scenario in Fig 4.2 and at a gradient of 230 T/m. These results were compared to results from a similar analysis for the lens operating under the antiproton-production mode of a gradient of 670 T/m at a pulse rate of 0.5 Hz [12]. Figure 4.16 (left) shows the ANSYS output thermal profile of a cutaway of the lens operating at 12 Hz. The lithium body corner is a temperature-sensitive location and should avoid lithium melting temperatures of 453.75 K. The corner temperature reaches a maximum temperature of 376 K. The plot on the right of Fig. 4.16 is the increase in maximum temperature of the lithium over the 16 pulses, depicting a change in temperature of 22 K when the operating temperature has come to equilibrium. We conclude from this analysis that the lithium lens is adequately cooled to operate at the nominal ($g - 2$) pulse rate.

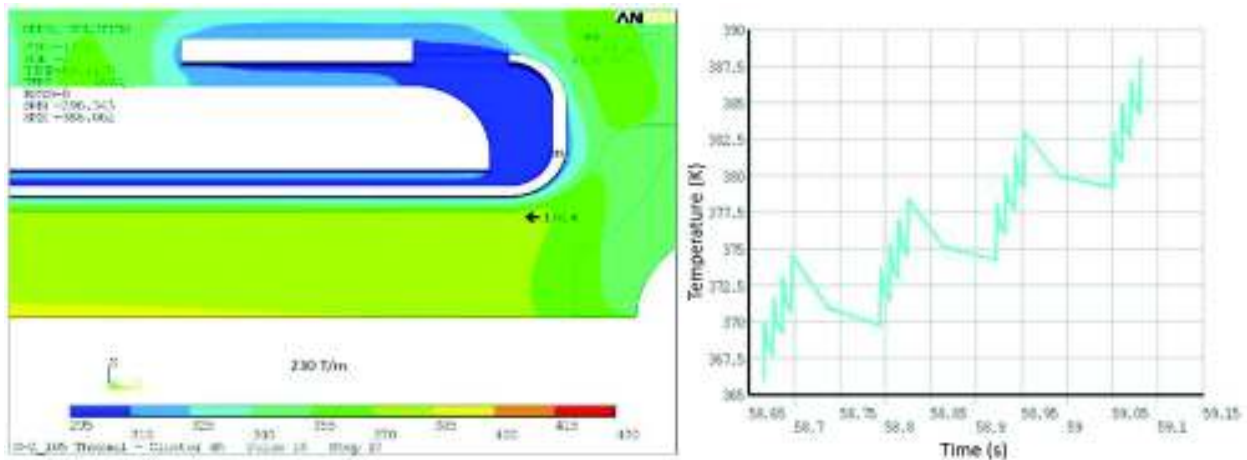


Figure 4.16: Simulated thermal profile from ANSYS for the lens operating at an average pulse rate of 12 Hz (left) depicting little beam heating and a corner temperature of 376 K. (Right) Plots showing lens temperature increase over the 16 pulses.

Mechanical fatigue was also assessed for the lithium lens. Figure 4.17 depicts a constant life fatigue plot developed for the lens from the ANSYS analysis. The two red lines represent upper and lower estimates of fatigue limits for the lens material. The red data points represent fatigues for gradients of 1000 T/m, 670 T/m, and two points at 230 T/m for a preload pressure of 3800 and 2200 psi, respectively. For the lens operating in the antiproton production conditions of 670 T/m, the mechanical fatigue was a large concern in the lens design. It appears that for the ($g - 2$) case, the mechanical fatigue will be a comparatively small concern.

This initial assessment of the lithium lens suggests that it should be able to operate at the ($g - 2$) repetition rate. However, since the operation of the lithium lens at the average 12 Hz rate is crucial, testing of the lens at 12 Hz is needed. Currently the lens is being pulsed in a test station at a 12 Hz rate in order to confirm that 1M pulses per day can be achieved and sustained over many months. Also, data from these tests can be used to confirm predictions of the ANSYS model.

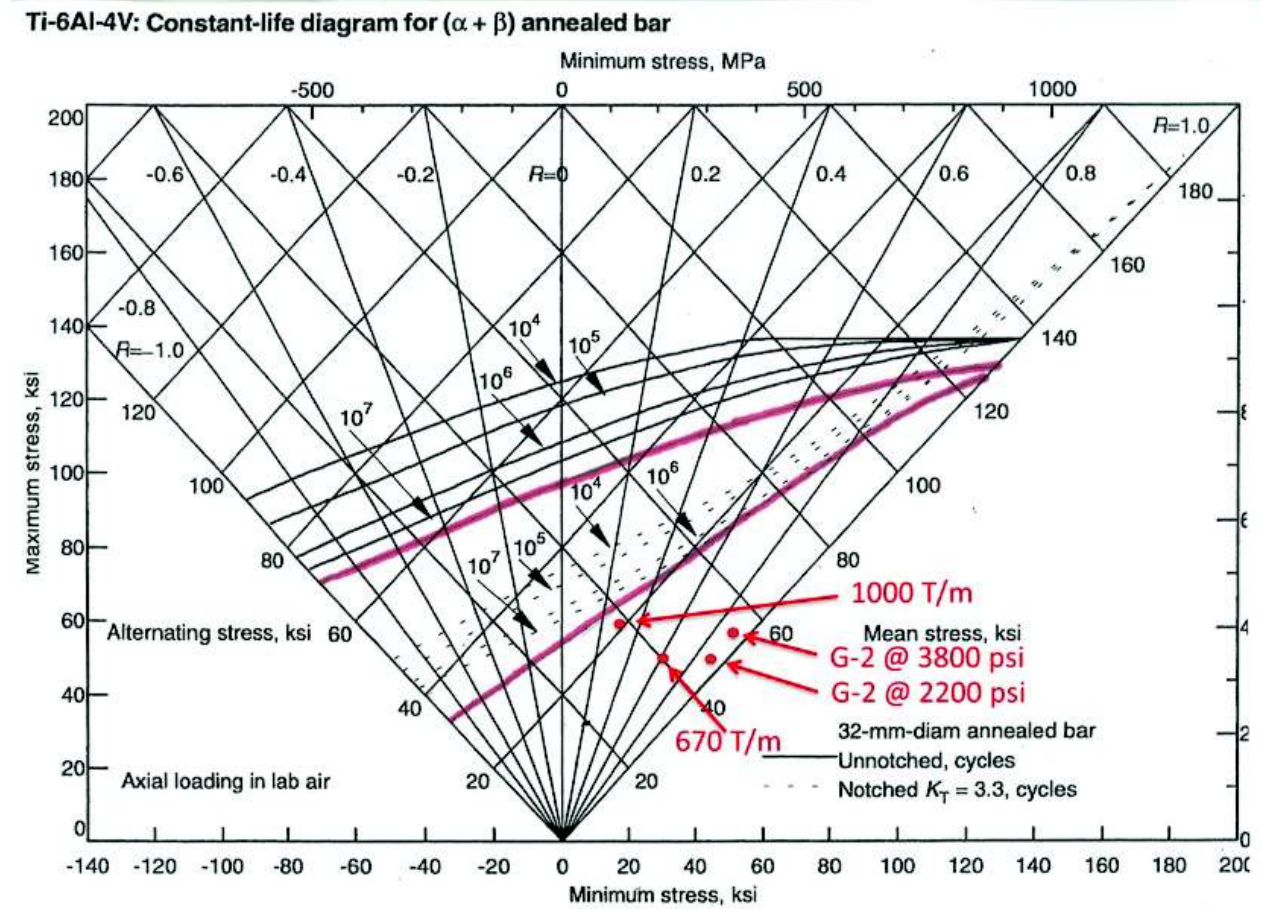


Figure 4.17: Constant-life fatigue plot of the lithium lens for antiproton and ($g - 2$) modes showing that mechanical fatigue for the ($g - 2$) pulse rate is a small concern.

4.4.3 Pulsed magnet (PMAG) and collimator

The pulsed magnet, shown in Fig. 4.18, selects 3.115 GeV/c positive particles and bends them 3° into the channel that begins the M2 beam line. The magnet will operate with a field of 0.53 T and is a 1.07 m long magnet with an aperture of 5.1 cm horizontally and 3.5 cm vertically. It is a single-turn magnet that has incorporated radiation-hard hardware such as ceramic insulation between the magnet steel and the single conductor bars, as well as Torlon-insulated bolts [10]. The pulsed magnet has a typical pulse width of $350 \mu\text{s}$ and similarly to the lithium lens, will need to accommodate the $(g - 2)$ pulse rate shown in Fig. 4.2. The pulsed magnet is water cooled. In addition to the magnet currently in the target vault, there are three spares.

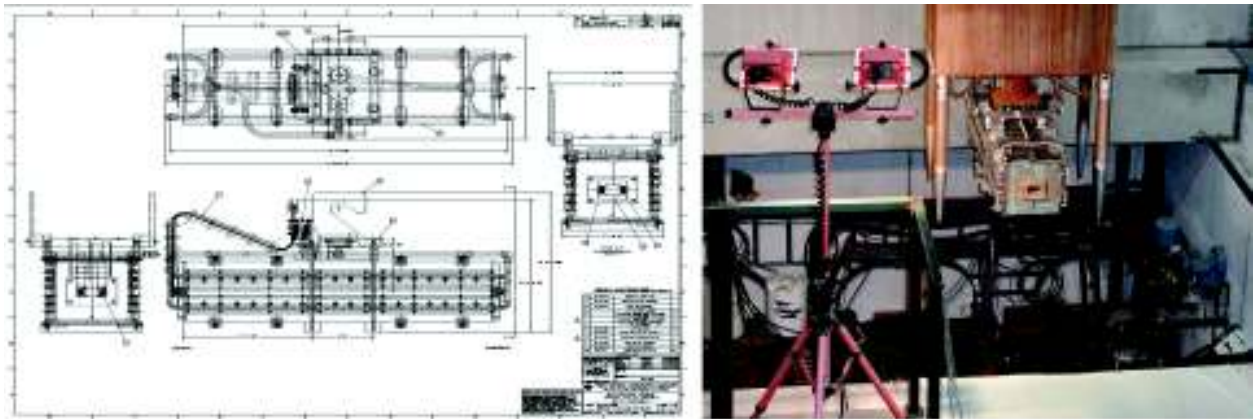


Figure 4.18: Pulsed magnet (PMAG) used for momentum-selection of pions.

One consideration that may require a change to the pulsed magnet design is the fact that the polarity of the selected particles for $(g - 2)$ is opposite that for antiproton production. MARS results predict that in the $(g - 2)$ polarity, a negatively-charged particle may interact with the downstream end of the magnet, increasing the integrated radiation dose. MARS simulations estimate the integrated dose at the downstream end of PMAG to be down by a factor of 5 compared to the antiproton production case, but the repetition rate is increased by a factor of 24. Therefore, a new magnet design may be required. A C-magnet style pulsed magnet would prevent the negative particles from hitting the pulsed magnet thus reduce the likelihood of magnet failures.

In order to accommodate the $(g - 2)$ pulse rate, the pulsed magnet power supply will also need to be modified or replaced with one similar to the new supply for the lithium lens with improved charging capability.

The collimator is located directly upstream of the pulsed magnet. The purpose of the collimator is to provide radiation shielding to the pulsed magnet to improve its longevity. It is a water-cooled copper cylinder 12.7 cm in diameter and 50.8 cm long. The hole through the center of the cylinder is 2.54 cm diameter at the upstream end, widening to a diameter of 2.86 cm at the downstream end. The existing collimator is currently planned to be used without modification.

4.4.4 Target station beam dump

The target-station beam dump absorbs particles which are not momentum-selected by the pulsed dipole magnet and continue straight ahead. The location of the beam dump can be seen in Fig. 4.19. The current beam dump has a graphite and aluminum core which is water cooled, surrounded by an outer steel box. The graphite core is 16 cm in diameter and 2 m in length, and is designed to handle a beam power of 80 kW [13]. The existing dump has a known water leak that developed at the end of the collider run. Therefore, consideration for replacing the beam dump will need to be made. The current plan is to replace the beam dump with an updated copy of the 80 kW beam dump. The maximum estimated beam energy load for $(g - 2)$ would occur if $(g - 2)$ takes advantage of extra cycles, running at a rate up to 18 Hz, during a hypothetical period when the NO ν A experiment would not be able to operate, and would be 25 kW, which is easily accommodated with the current dump design.

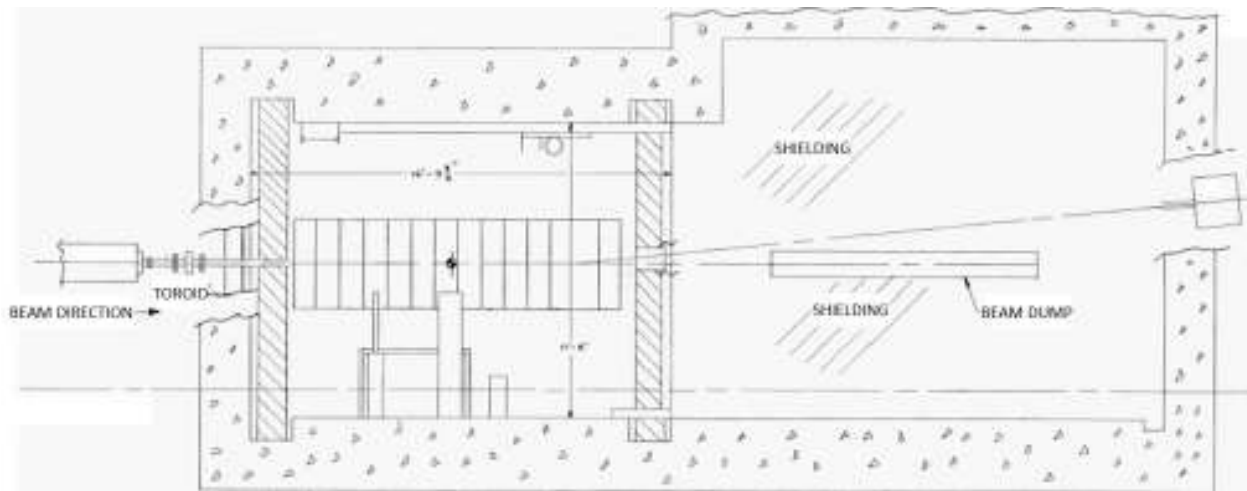


Figure 4.19: Layout of the target-station beam dump.

An alternative, shorter, cost-effective dump was also considered and designed at an operating capacity of 25 kW. This design resulted in a copper cylinder 2 ft long and 6 in in diameter, with copper cooling tubes vacuum-brazed around the outside of the cylinder (Fig. 4.20).

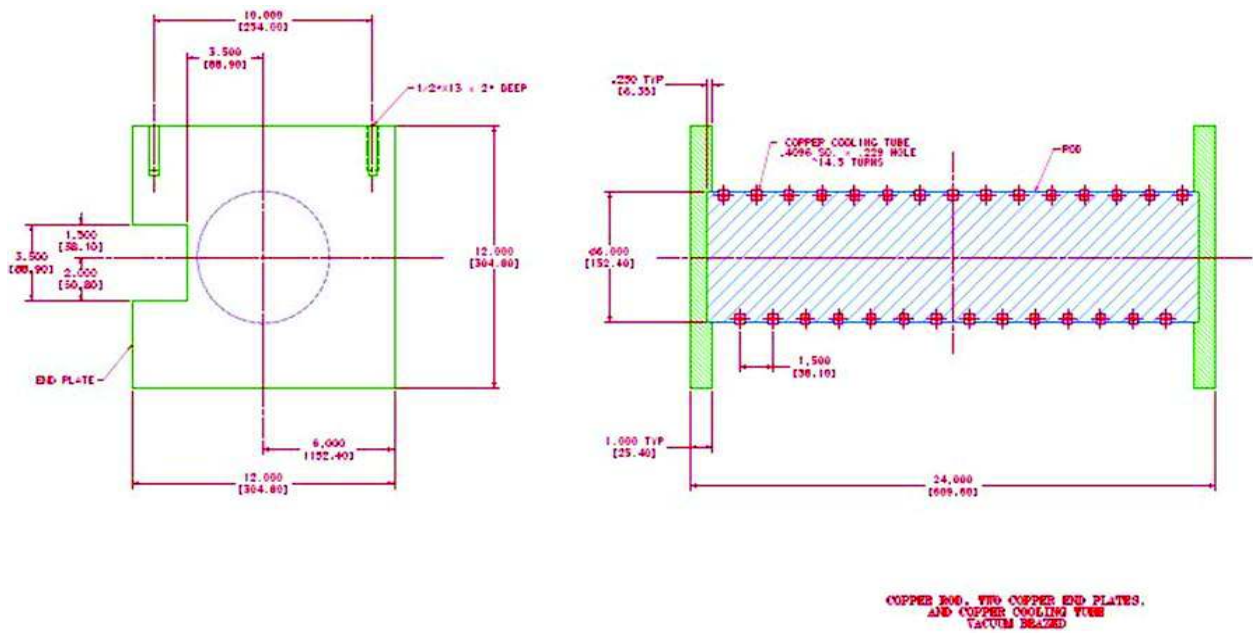


Figure 4.20: Alternate 25 kW dump made of a copper-core rod with copper water tubing for cooling.

4.5 Beam Transport Lines

4.5.1 Overview of $(g - 2)$ beamlines

The existing tunnel enclosures and beamlines connecting the Recycler Ring to the Delivery Ring will be largely reused for $(g - 2)$ operation. However, there are fundamental differences between the way the Rings and beamlines were operated for Collider Operation and how they will be used to support the Muon Campus. A high-intensity, 8 GeV kinetic energy proton beam will be transported to the AP0 Target Station in $(g - 2)$ operation and to the Delivery Ring for the Mu2e experiment. The increase in intensity from Collider Operation in conjunction with the beam size of the 8 GeV beam will present challenges for efficient beam transfer. The beamlines downstream of the AP0 Target Station will need to be reconfigured to connect to the D30 straight section of the Delivery Ring. New extraction lines will be constructed to transport beam from the D30 straight section to the $(g - 2)$ and Mu2e experiments. Careful planning is required for the D30 straight section of the Delivery Ring due to the presence of both the injection and extraction points. The extraction line will also need to support both single-turn extraction for $(g - 2)$ and resonant extraction for Mu2e.

4.5.2 Beamline Changes from Collider Operation

During Pbar operation in Collider Run II, the P1 line connected to the Main Injector at the MI 52 location. The P1 line supported operation with three different beam energies, 150 GeV for protons to the Tevatron, 120 GeV for Pbar production and SY120 operation, and 8 GeV for protons and antiprotons to and from the Antiproton Source. The junction between the P1 and P2 lines occurs at F0 in the Tevatron enclosure. The P2 line ran at two different beam energies, 120 GeV for antiproton production and SY120 operation and 8 GeV for protons and antiprotons to and from the Antiproton Source. The P2, P3 (for SY120 operation), and AP-1 lines join at the F17 location in the Tevatron enclosure. The AP-1 line also operated at 120 GeV and 8 GeV, but is not used for SY120 operation. The AP-3 line only runs at a kinetic energy of 8 GeV. The AP-3 line connects with the AP-1 line in the Pre-Vault beam enclosure near the Target Vault and terminates at the Accumulator.

After the conversion from collider to NO ν A and $(g - 2)$ operation, the Recycler will become part of the proton transport chain and will connect directly with the Booster. There will be a new beamline connection between the Recycler Ring and the P1 line. The P1 line will become a dual energy line, with no further need to deliver 150 GeV protons with the decommissioning of the Tevatron. The P2 line will continue to operate at both 8 GeV for the Muon experiments and 120 GeV for SY120 operation. The AP-2 and AP-3 lines will need to be almost completely dismantled and reconfigured to support both the transport of muon secondaries via the Target Station for $(g - 2)$ and protons via the target bypass for Mu2e. The $(g - 2)$ 3.1 GeV secondary beamline emanating from the Target Station and the Mu2e 8 GeV primary beamline bypassing the Target Station will merge and follow a single line to the Delivery Ring. The new injection line will connect to the Delivery Ring in the D30 straight section. The extraction line also originates in the D30 straight section and has to be capable of supporting both resonant and single-turn extraction.

The beamlines that made up the Antiproton Source, those that have an “AP” prefix,

will be modified, reconfigured and renamed prior to $(g - 2)$ operation. The AP-1 line will only operate at an energy of 8 GeV and will be renamed M1. The AP-1 line will be largely unchanged, with the exception of the replacement of some magnets to improve aperture. The AP-2 line will become two separate beamlines and no longer be continuous. The upstream end of the line is needed as a pion decay channel for the $(g - 2)$ experiment and will be renamed M2. It will provide a connection from the Pbar AP0 Target Station to the M3 line. The downstream section of AP-2 will become the abort and proton removal line from the Delivery Ring. The old AP-3 line will be required to transport both 8 GeV beam for the Mu2e experiment and also a 3.1 GeV secondary beam for the $(g - 2)$ experiment and will be renamed M3. The 18.5° right bend will be changed from a two to a three dipole configuration in order to avoid higher beta functions in this region. The M3 line will also be modified to connect to the Delivery Ring (formerly Debuncher) instead of the Accumulator. The extraction line connecting the Delivery Ring to the experiments will be called M4. The $(g - 2)$ line will branch from the M4 line in the “Left Bend” area. Figure 4.21 compares the Pbar beamline configuration with that proposed for $(g - 2)$ and Mu2e operation. In general, the AP-1, AP-2 and AP-3 lines will refer to the old Pbar beamline configuration and M1, M2, M3, M4 and $g - 2$ will refer to the beamline configuration for $(g - 2)$ operation.

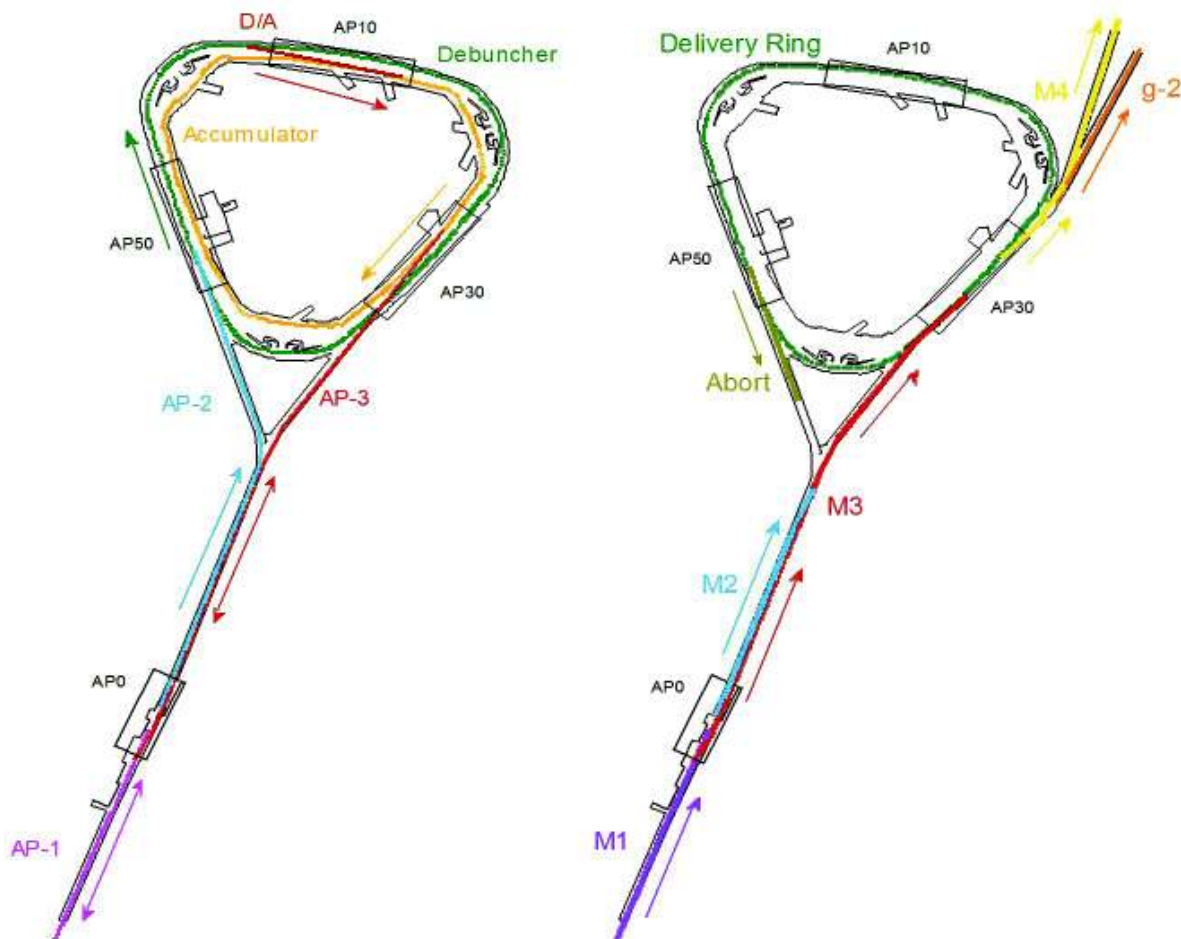


Figure 4.21: Layout of the Antiproton Source beamlines (left) and the reconfigured beamlines for $(g - 2)$ operation (right).

Most of the common improvements to the beamlines and Delivery Ring that benefit Mu2e, $(g - 2)$, and future experiments will be incorporated into an Accelerator Improvement Project (AIP). Table 4.4 summarizes which improvements are contained in the AIP, as well as those that will be managed as part of the Recycler Ring AIP, Mu2e and $(g - 2)$ projects. Project Managers for the various projects will work closely together to ensure they interface properly. Virtually all of the work that is incorporated into the AIP's must be completed prior to beam operation to $(g - 2)$.

Description	Project	Comment
Recycler RF upgrade	RR AIP	
Recycler extraction/P1 stub line	RR AIP	
P1,P2 and M1 aperture upgrade	DR AIP	M1 final focus quadrupoles are $(g - 2)$
Reconfigure AP-2 and AP-3	$(g - 2)$	New lines are called M2 and M3
Final focus to AP0 Target Station	$(g - 2)$	
AP0 Target Station upgrades	$(g - 2)$	
Beam transport instrumentation	DR AIP	
<i>Beam transport controls</i>	<i>Mu2e</i>	
Beam transport infrastructure	DR AIP	
Delivery Ring injection	DR AIP	
D30 straight section preparation	DR AIP	
Delivery Ring modification	DR AIP	
D.R. abort/proton removal	DR AIP	
<i>Delivery Ring RF system</i>	<i>Mu2e</i>	
<i>Delivery Ring controls</i>	<i>Mu2e</i>	
Delivery Ring instrumentation	DR AIP	<i>DCCT and Tune measure are Mu2e</i>
<i>Resonant extraction from DR</i>	<i>Mu2e</i>	
Fast extraction from DR	$(g - 2)$	
Delivery Ring infrastructure	DR AIP	
Extraction line to split	$(g - 2)$	Upstream M4 line
<i>Extraction line from split to Mu2e</i>	<i>Mu2e</i>	<i>Downstream M4, including extinction</i>
Extraction line from split to $(g - 2)$	$(g - 2)$	Beamline to MC-1 building

Table 4.4: Beam-line and Delivery-Ring upgrades and associated project: $(g - 2)$ project, Mu2e project, Delivery Ring Accelerator Improvement Project (DR AIP), and Recycler Ring AIP (RR AIP).

4.5.3 Proton Beam Transport to the Target Station

Beam transport of the 8 GeV primary beam from the Recycler Ring (RR) to the Target Station closely resembles the scheme used to transport 120 GeV protons for antiproton production in Collider operation. The most notable differences are the change in beam energy and the switch from the Main Injector to the RR as the point of origin for the P1 line. The beamlines will be modified to 1) provide a connection between the RR and P1 line, 2) improve aperture to accommodate the larger beam size and intensity, and 3)

reconfigure the final focus region in order to reach the desired spot size on the production target. Table 4.5 lists the beamlines connecting the RR with the Target Station and their respective lengths.

Beam Line	Length (m)
RR to P1	43
P1	182
P2	212
AP-1 (M1)	144
RR to Target Total	581

Table 4.5: Recycler Ring to Target beam line lengths.

Recycler Ring to P1 line stub

Operation of $(g - 2)$ and Mu2e requires the transport of protons from the RR rather than the Main Injector. A new transfer line from the RR to the P1 beamline will be constructed to facilitate proton beam transport from the RR to the Delivery Ring. This new beamline provides a way to deliver 8 GeV kinetic energy protons to the Delivery Ring, via the RR, using existing beam transport lines and without the need for new civil construction.

Beamline Design The P1 line is lower in elevation than the RR, thus the beam will be extracted downward. This will be accomplished with a horizontal kicker that will displace beam into the field region of a Lambertson magnet that will bend beam down. The kickers are located immediately downstream of the RR 520 location and the Lambertson will be just downstream of the RR 522 location. Due to space limitations, only two vertical bend centers made up of the Lambertson and a dipole are used in the new line. An integer multiple of 360° in betatron phase advance between the two bending centers is required to cancel the vertical dispersion from the bends. The new beamline needs to intercept the existing P1 line in a location that doesn't disturb the extraction trajectory from the Main Injector, which will be retained for SY120 operation. That junction point will be located near quadrupole Q703. The angles of both the Lambertson and the vertical bending magnet (VBEND) were obtained by matching the site coordinates from the RR to P1 line using TRANSPORT [14] code. Figure 4.22 shows the layout of the new line, with the existing P1 line drawn in red.

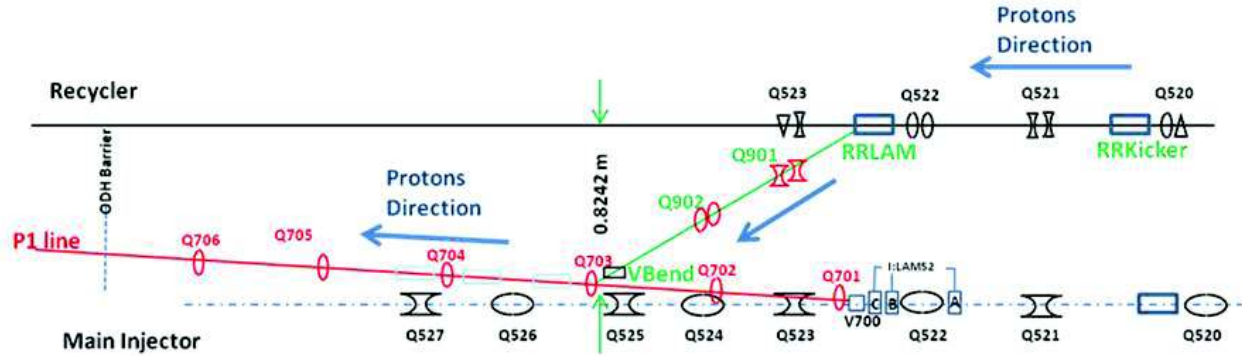


Figure 4.22: The new Recycler Ring to P1 connecting beamline.

Kickers The $(g - 2)/\text{Mu}2e$ extraction kicker will be of the same design as the kickers used during collider operation, but will be potted instead of using Fluorinert for electrical insulation. The physical dimensions and properties of the kickers are listed in Table 4.6. The plan is to reuse the ceramic vacuum chamber from old RR kicker magnets, which are slightly smaller than the standard RR vacuum chamber. The kicker system will be made up of two magnets producing 0.79 mrad each for a total kick of 1.58 mrad. The new kicker power supplies will be located in the MI-52 service building. Power supplies for the new beamline magnets will also be located at MI-52. This service building will be expanded to accommodate the new power supplies.

Recycler Extraction Kicker RKB-25	
Parameter	Value
Ferrite length	46.6 in
Case length	64.0 in
Insert length	67.78 in
Print number	ME-481284
Maximum strength (each)	0.279 kG m
Maximum kick (each)	0.94 mrad @ 8 GeV/c ²
Required kick (each)	0.79 mrad @ 8 GeV/c ²
Rise time, 3% - 97%	140 ns

Table 4.6: RR extraction kicker parameters.

Lambertson The Lambertson magnet will be rolled 2.7° and the vertical bend magnet -4.0° to provide a small horizontal translation in order to create the proper horizontal trajectory required to match the P1 line. The vertical dipole magnet is a 1.5 m “modified B-1” type that will provide a 21 mrad bend, matching the bend of the Lambertson. There will be two quadrupoles located between the Lambertson and vertical dipole magnets that make up the dogleg between the RR and P1 line. Due to space constraints, the quadrupoles are shifted downstream from their ideal locations by 0.25 m. A more detailed technical descrip-

tion of the design features of the new beam line stub can be found in Ref. [15]. Figure 4.23 shows the lattice functions for the entire RR to Target Station line.

Figure 4.23: LATTICE FUNCTIONS FOR RR TO TARGET STATION

Recycler orbit The RR extraction scheme incorporates a permanent horizontal 3-bump in the RR that displaces the circulating beam outward 25 mm at the upstream end of the Lambertson (RLAM). Figure 4.24 shows the trajectories of the circulating and extracted beams, including the horizontal bump at the Lambertson. The bump is created by horizontal trim dipoles at the 524, 522 and 520 locations. The extraction kickers displace the extracted beam inward 25 mm at the same location. This creates a separation of the RR circulating beam and extracted beam at the front face of the Lambertson of 50 mm.

Apertures Lambertson magnets are typically one of the limiting apertures in a beamline. The Recycler extraction Lambertson has an adequate aperture for both the circulating and extracted beams. Figure 4.25 shows the footprint of both beams at the Lambertson for both a 10σ and 6σ beam size. The vertical bend magnet has a relatively small horizontal aperture, but is located where the horizontal beta functions are small. The horizontal acceptance of the vertical dipole is actually larger than that of the Lambertson, despite the smaller physical aperture. The quadrupole and trim magnets are modeled after those in the Recycler and have good apertures.

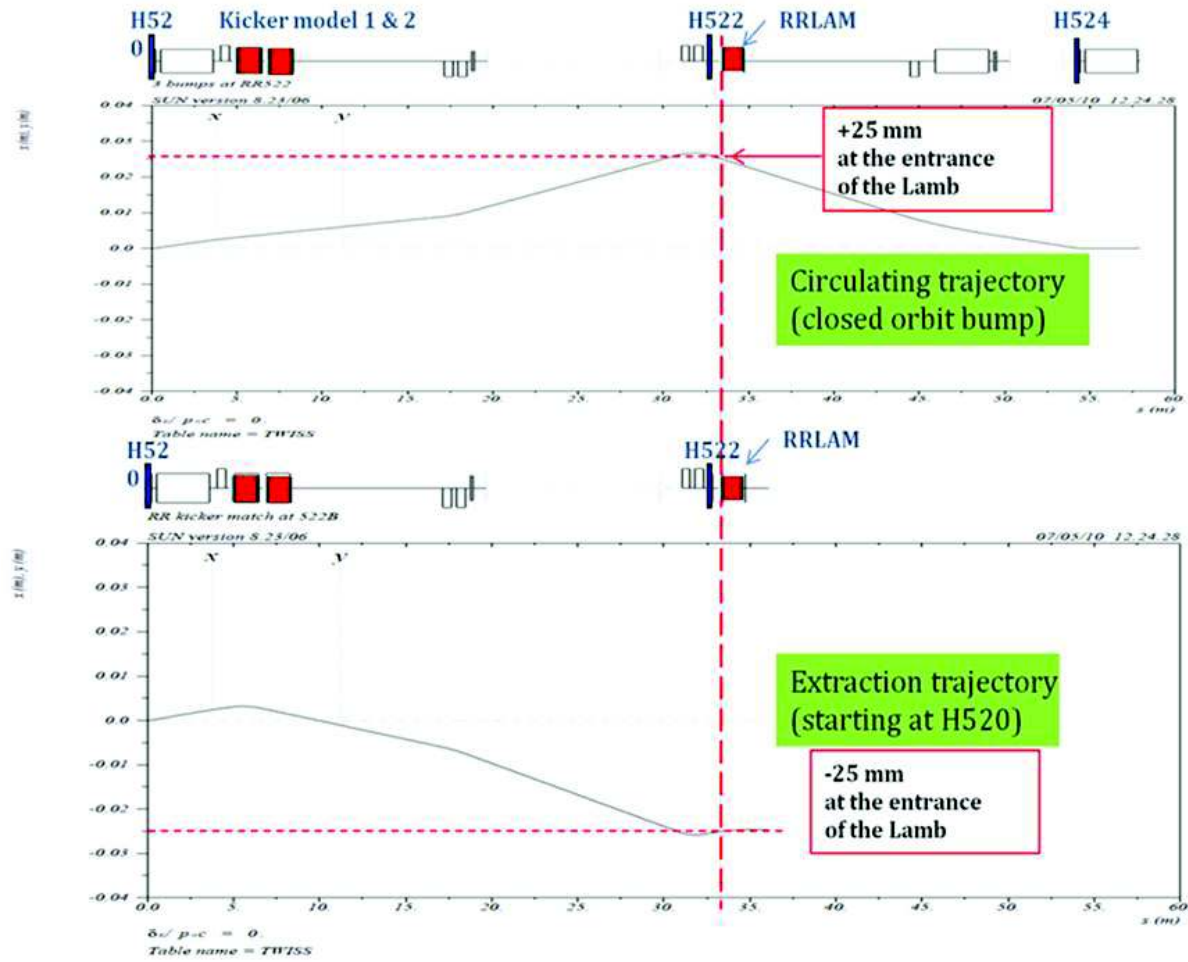


Figure 4.24: Horizontal trajectories for circulating and extracted beam from the RR.

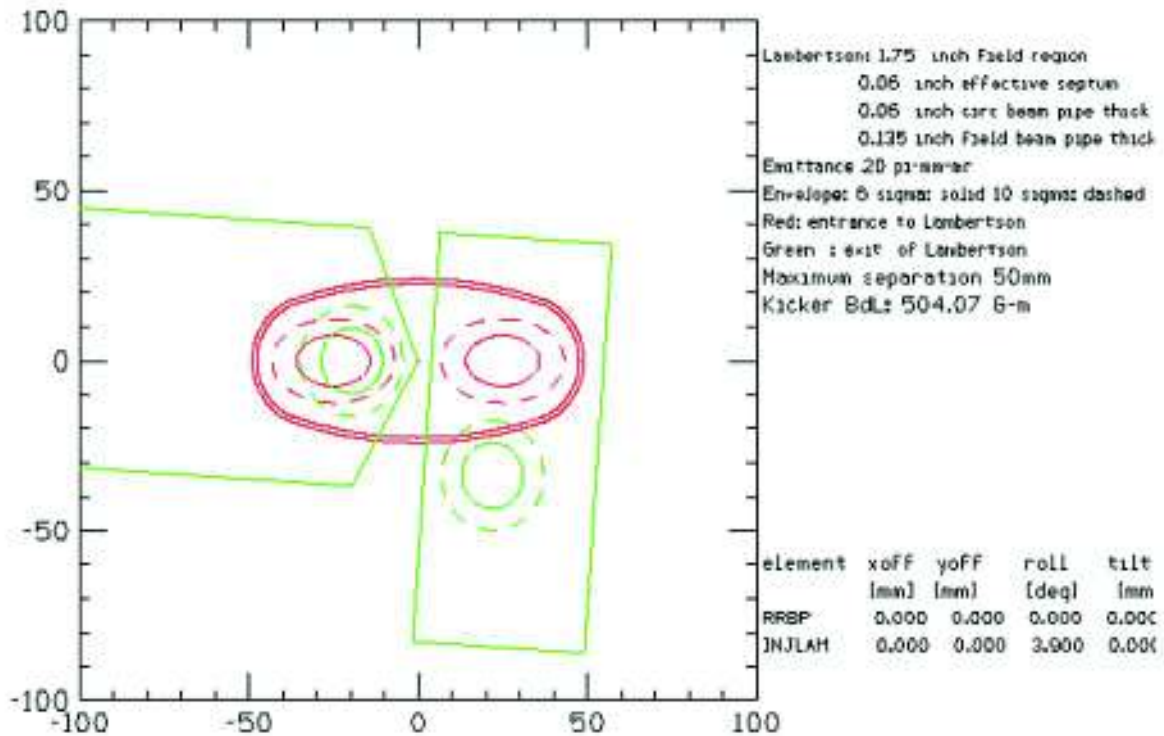


Figure 4.25: Beam sizes at the entrance (red) and exit (green) of the extraction Lambertson. The dashed outline represents 10σ and the solid outline 6σ beam for a normalized emittance of 18π -mm-mrad.

4.5.4 P1, P2 and AP-1 Aperture Improvements

The increased intensity and beam size planned for muon operation will lead to unacceptably high beam loss unless apertures are improved in the P1, P2 and AP-1 lines. Limiting apertures were identified during Collider Run II when evaluating possible improvements, simplifying the process of identifying locations. The elimination of AP-1 120 GeV operation for antiproton stacking provides an opportunity to improve the aperture with weaker magnets that previously were not practical for use as replacements.

The introduction of the P1-line stub has eliminated several aperture restrictions that were associated with Main Injector extraction. In particular, the vertical C-magnets that follow the MI-52 Lambertson will be avoided with the new stub line. Most of the P1 line after the P1-line stub has good aperture, until the former junction area with the Tevatron. The vertical dipole at the 714 location was installed as a C-magnet because of its proximity with the Tevatron and has a small horizontal aperture. The decommissioning of the Tevatron allows the replacement of this magnet with a conventional dipole that will increase the horizontal acceptance by more than 50%. The new magnet must also be capable of producing enough field strength to operate at 120 GeV and support SY120 operation. The four Tevatron F0 Lambertsons will no longer be needed to inject protons into the Tevatron and can be removed to improve the aperture, also in the horizontal plane.

In addition to the improvements to physical aperture, a new quadrupole is proposed in the region presently occupied by the Tevatron injection Lambertsons at F0. The long drift space in the P1 and P2 lines required for Tevatron injection results in large excursions in dispersion throughout the beamlines. Unless the dispersion is reduced, the increased momentum spread created by RR bunch formation will cause high beam losses. The addition of a quadrupole (or quadrupoles) in this region will provide the means to improve the optics of the transport lines.

The P2 line will remain a dual-energy line supporting $(g - 2)$ and SY120 operation, so the junction between the P2, AP-1, and P3 beamlines at F17 will remain. The aperture for both $(g - 2)$ and SY120 operation will substantially improve with the proposed replacement of the F17 C-magnets with a large aperture CDA magnet that both beams will pass through. The B-3 dipole at the F-17 location will remain.

AP-1 will only operate at 8 GeV for $(g - 2)$ operation, so the eight EPB magnets that make up the HV100 and HV102 string can be replaced with larger, weaker dipoles. The number of dipoles can be reduced from four to two in each string. The 1.5 m “modified B-1” magnets (formally known as MDC magnets) have a pole gap that is 2.25 in instead of 1.5 in and provides more than a factor of two increase in acceptance. Several trims will also be replaced or relocated to complete the aperture upgrade. The final-focus region at the end of AP-1 is described separately in the next section. Table 4.7 summarizes the proposed improvements to the physical apertures in the RR to Target Station lines. Reference [15] has a more detailed explanation of the devices used to improve the aperture and how the improvements will be implemented.

Location	Existing magnet	Proposed improvement
V714	C-magnet	1 B2 magnet
F0 Lambertsons	4 Lambertsons	Remove magnets
F17 (V)	B3 and two C-magnets	1 CDA (retain B3)
HV100	4 EPB dipoles	2 MDC
HV102	4 EPB dipoles	2 MDC

Table 4.7: Proposed aperture improvements for RR to Target Station beamlines.

Final Focus Region

The desired spot size on the production target, a proton beam σ in both planes of 0.15 mm, is the same as what was used in antiproton production during collider operation. Because the beam momentum is 8.89 GeV/c for ($g - 2$) operation instead of the 120 GeV/c that was used for antiproton production, much smaller beta functions are required to achieve this spot size (0.068 m vs. 0.878 m, respectively). The larger beam size would also lead to beam loss and reduced transfer efficiency with the existing quadrupole magnets and lattice, due to their aperture, length, and busing configuration. The existing quadrupoles in the AP-1 line are 3Q120 magnets that are 120 in (3.048 m) long and have a 3 in (76 mm) circular aperture. One advantage that the reduced beam momentum provides is the greatly reduced quadrupole gradients required to focus the beam. Figure 4.26 shows a modified version of the scheme proposed in Ref. [16], where a quadrupole triplet replaces the last quadrupole, PQ9B, in the AP-1 line. Figure 4.26 shows the optics in the final 50 m of the AP-1 line where the final focus occurs. The PQ8A&B and PQ9A magnets are not powered and can be removed to improve aperture, if desired. The peak beta functions in the quadrupole triplet are reduced by shifting the magnets as close to the vault wall as possible. By removing the Beam Sweeping system used in Pbar operation and relocating toroid TOR109, the triplet can be shifted by more than 2 m (this configuration is shown in Fig. 4.26). It is also advantageous to use shorter quadrupole magnets in the triplet as another means of locating the magnets further downstream. There are two magnet options using available magnets that are under consideration. Both are relatively compact and have adequate apertures. The first is a 4Q16 – 4Q24 – 4Q16 (from BNL) grouping and the other is made up of an SQA – SQC – SQA (Pbar) combination. Even without the shorter magnets, the desired spot size of $\sigma_x = \sigma_y = 0.15$ mm can be achieved at the production target.

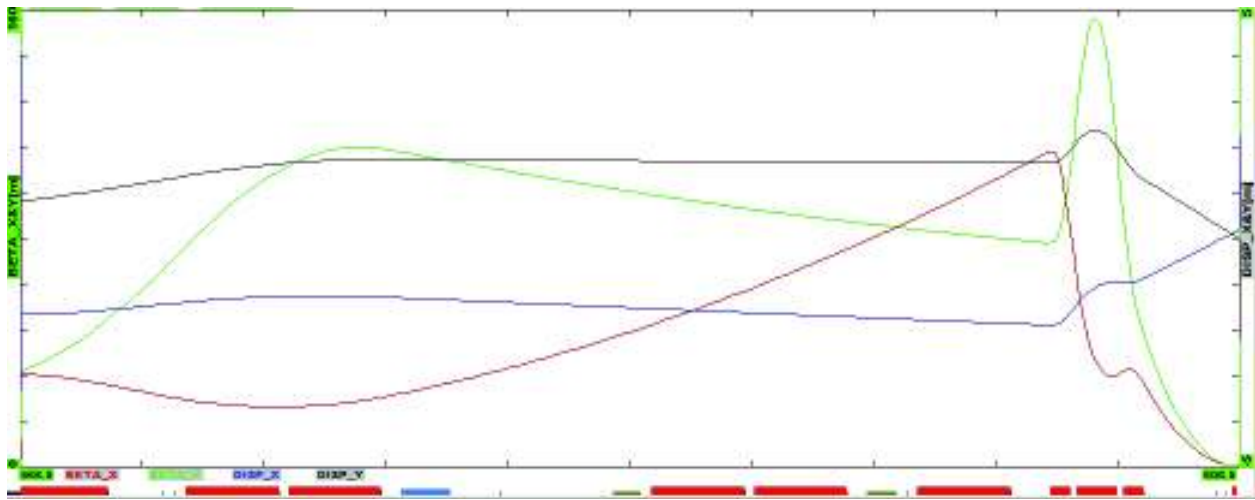


Figure 4.26: Beta functions (horizontal is red, vertical is green) and dispersion functions (horizontal is blue, vertical is black) for final focus region of AP-1 line.

4.5.5 Pion to muon decay beam lines

4.5.6 Delivery Ring

The Pbar Debuncher ring will largely remain intact for $(g-2)$ operation and will be renamed the Delivery Ring for its new role in providing muons to the experiment. A considerable amount of equipment left over from Pbar operation will need to be removed from the Debuncher. Most of the equipment targeted for removal was used for stochastically cooling the antiproton beam during collider operation and is not needed for $(g-2)$. Some of these devices also have small apertures, so the ring acceptance will be improved with their removal. The cooling tanks in the D30 straight section also need to be removed to provide room for the new injection and extraction devices.

The Pbar Accumulator ring will not be needed for $(g-2)$ and Mu2e operation and will become a source of magnets, power supplies and other components for use in the reconfigured beamlines. In particular, the M4 (extraction) line will be largely made up of former Accumulator components. Some larger-aperture magnets will also be needed in the injection and extraction regions and will come from the Accumulator or other surplus sources.

Rings Lattice and Acceptance

The original design lattice for the Debuncher will be used for the Delivery Ring with few modifications. The lattice has a 3-fold symmetry with additional mirror symmetry in each of the three periods, with three zero-dispersion straight sections: D10, D30 and D50. The original lattice parameters were largely dictated by the requirements for Pbar stochastic cooling and the RF systems. The Debuncher was designed with a large transverse and longitudinal momentum acceptance in order to efficiently RF-debunch and stochastically cool antiprotons from the production target. This lattice design is also well suited for $(g-2)$ operation. During Collider Run II, the original lattice was distorted somewhat in order to reduce the beam size in the stochastic cooling tanks that had limiting apertures. Since these tanks will be removed, the lattice that will be used for the $(g-2)$ conceptual-design work will revert back to the original Debuncher design lattice. Figure 4.27 shows the lattice functions for one period of the Debuncher.

It should be noted that the design acceptance of the Debuncher was 20π -mm-mr. During the 25 years of Pbar operation, numerous aperture improvements were undertaken to boost the acceptance of the Debuncher. After the final Collider Run II aperture improvements were put in place in 2007, the measured acceptance of the Debuncher was as high as 33π -mm-mr in both transverse planes. The $(g-2)$ design goal of a 40π -mm-mr acceptance for the Delivery Ring, while reusing as much of the original equipment as possible, presents a difficult challenge.

The transverse acceptances of the Debuncher dipole, quadrupole, sextupole, and trim magnets are quite large. The smallest magnet acceptance is in the vertical plane of the dipoles and is approximately 54π -mm-mr on one end, growing to 79π -mm-mr on the other end. The dipoles have a 90π -mm-mr or larger horizontal acceptance (90π -mm-mr for the $\pm 2\%$ momentum spread and locations with the largest dispersion) and the other magnets have a 100π -mm-mr or larger acceptance in both planes. Since the original Debuncher lattice will not be significantly changed for $(g-2)$ operation, the main Delivery-Ring magnets will

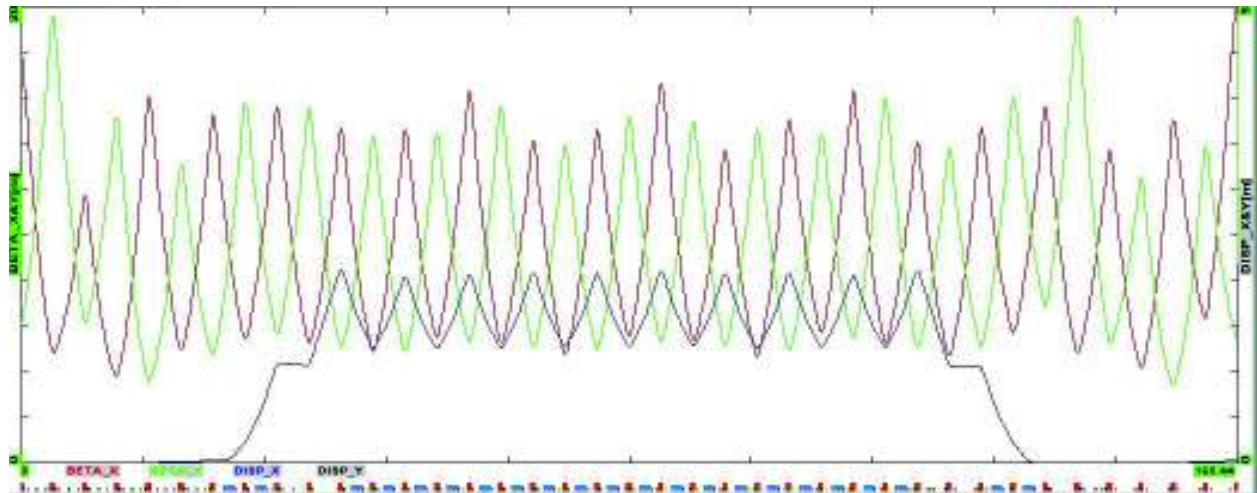


Figure 4.27: Debuncher/Delivery Ring lattice functions through 1/3 of the ring. β_x is in red, β_y in green, and horizontal dispersion in blue.

not be limiting apertures. In general, devices with a physical aperture of 50 mm or greater provide an acceptance of over 40π -mm-mr in the Debuncher, and select locations can provide that acceptance for devices that have an aperture of 40 mm, as long as they are relatively short.

During Collider operation, the smallest physical apertures in the Debuncher came from stochastic cooling tanks, RF cavities, instrumentation, and devices used for injecting and extracting beam. Many of these devices will be removed as part of the repurposing of the Debuncher for the muon experiments. Some of these devices, most notably the kickers, will be retained in the interest of economy and/or complexity and lead-time of manufacture. Other devices, such as the injection septa, will be new devices with necessarily small physical apertures in order to provide enough bend strength.

During Collider Run II, the Band-4 stochastic cooling tanks were the limiting aperture in both planes of the Debuncher. The Band-4 tanks had a 38 mm physical aperture in the cooling plane, and there were both horizontal and vertical pick-up and kicker tanks in the D10 and D30 straights respectively. All of the stochastic cooling tanks will be removed prior to $(g - 2)$ operation.

There is only one RF cavity planned for the Delivery Ring, which is needed to support Mu2e operation and will have an aperture similar to the Debuncher rotator cavities. Since the rotator cavities had an acceptance that was greater than 100π -mm-mr, the new cavity will have ample aperture and need not be removed when switching from operating Mu2e to $(g - 2)$. All RF cavities used for antiproton production will be removed prior to $(g - 2)$ operation.

Many of the beam detectors used during Pbar operation had small physical apertures in order to improve sensitivity. Since the beam intensities when running $(g - 2)$ are expected to be even smaller than those seen during Pbar operation, designers will need to be mindful of the aperture needs of the $(g - 2)$ experiment. Similarly, when instrumentation is being considered for reuse in the Delivery Ring, the physical aperture and proposed tunnel location should be analyzed for adequate acceptance.

The transverse Schottky detectors used in the Debuncher had apertures that were only slightly larger than the Band-4 stochastic cooling pick-up. They were removed from the Debuncher during Run II, but have been reinstalled for use during $(g - 2)$ and Mu2e studies. Although these Schottkys are slated for removal prior to $(g - 2)$ operation, the Mu2e experiment may need a new device to monitor tunes during resonant extraction. If a new device is made, it will need to have adequate aperture for $(g - 2)$ or will have to be removed when switching between the two experiments. The DCCT beam-intensity monitor will also be used by the Mu2e experiment. It is expected to have adequate aperture as long as it is located in the middle of a straight section half-cell, where the beam has a circular cross-section.

Both injection from the M3 line and extraction to the M4 line take place in the D30 straight section. Injection will be located in the upstream half of the straight section, and the pulsed magnetic septum and kicker magnets will have small apertures in order to provide adequate bending strength. The septum has a small aperture in both planes, while the kicker is primarily limited in the horizontal plane. The septum is a modified Booster-style (BSE) magnetic septum magnet. The septum modifications involve increasing the pole gap from 28 mm to 42 mm in order to greatly improve the horizontal acceptance, and reducing the septum thickness from 14 mm to 9 mm to increase the vertical acceptance. The injection kicker system will be made up of two surplus Pbar AP-4 injection kicker magnets. The horizontal aperture is only 41 mm and will likely be one of the limiting apertures of the Delivery Ring. The extraction kicker system will be made up of two Pbar extraction kicker magnets. They have a vertical aperture of 41 mm and will also be one of the limiting apertures of the Delivery Ring.

Kickers and Septa

The kickers and septa required for $(g - 2)$ operation will need to operate at a much higher frequency than that used for antiproton production, with peak rates increasing as much as a factor of 30. In an effort to make the new kicker systems more economical, existing kicker magnets will be reused. Kickers will be required for injection and extraction from the Delivery Ring as well as for proton removal. Table 4.8 compares kicker parameters for existing Pbar systems to the specifications for the $(g - 2)$ injection and proton-removal kickers. The rise and fall time specifications for $(g - 2)$ are less strict than what was needed for antiproton production, due to the short bunch length of the muons (and protons). Although the Pbar kicker magnets are suitable for reuse, new power supplies will be needed to operate at the increased rate. Resistive loads for the kickers will need to be cooled with Fluorinert. A single Fluorinert distribution system is planned, with piping bridging the distance between the load resistors from kickers in the 30 and 50 Straight Sections.

The septa and pulsed power supplies used during Pbar operation are not suitable for rapid cycling and cannot be used for $(g - 2)$. The septa have no internal cooling to handle the increased heat load from the planned high duty cycle, and the power supplies are not able to charge quickly enough. The Booster-style septum magnets can be modified to have the necessary size and field strength required for use in the injection and proton removal systems, and therefore are the preferred choice. The power supplies used in the Booster to power the septum magnets also appear to be a good fit. Although they are designed to operate at a lower frequency (15 Hz) than the peak needed for $(g - 2)$, the lower operating current

Kicker (modules)	Integrated Field (kG-m)	Kick Angle (mrad)	Rise Time 95%/5% (ns)	Fall Time 95%/5% (ns)	Flat Top Time (ns)
Debuncher Extraction (3)	1.34	4.6	150	140	1700
Debuncher Injection (3)	1.81	6.1	180	150	1700
Delivery-Ring Injection (2)	0.57	6.1	n/a	450	450
Delivery-Ring Extraction (2)	0.72	7.0	450	n/a	450
Delivery-Ring Proton Removal (3)	0.57	6.1	450	n/a	1700

Table 4.8: Existing Pbar (top) and future ($g - 2$) (bottom) kicker strength and waveform specifications.

(for 3.1 GeV/c versus 8.89 GeV/c momentum) should more than compensate for changes to the heat load and mechanical stresses due to the increased pulse rate. The Booster septum magnets are slightly shorter than their Pbar counterparts, so the new septa can fit where the Debuncher injection septum presently resides.

Delivery Ring D30 straight section

The Delivery-Ring injection and extraction regions will both be located in the D30 straight section. In both cases, the tight quadrupole spacing in the Delivery Ring creates physical conflicts with existing utilities and ring devices in the areas of elevation change to and from ring level. The existing cable trays on the Debuncher side of the ring will need to be completely dismantled and relocated towards the middle of the tunnel so that the new beamlines can be hung from the ceiling. The extraction line will closely follow the trajectory of the decommissioned AP-4 (Booster to Debuncher) line. The tunnel in this region has an existing stub region that the extraction line will pass through, eliminating the need for civil construction to widen and strengthen the tunnel. Figure 4.28 shows the layout of injection and extraction devices in the D30 straight section.



Figure 4.28: D30 straight section, injection on right, extraction on left.

Injection

The M3 line runs above the Delivery Ring in the upstream end of the D30 straight section and ends with a vertical translation into the ring. M3 injection will be achieved with a combination of a C-magnet, magnetic septum, D3Q3 quadrupole, and kicker magnets, which will all provide vertical bends. The septum and C-magnet are both based on existing designs, which reduces overall costs, but modified to improve the aperture. Both magnet designs required modifications in order to attain the ($g - 2$) acceptance goal of 40π -mm-mr.

The magnetic septum is a modified Booster-style (BSE) magnet, with an increased pole gap and a thinner septum to improve aperture. The BSE magnet has a 1.1-in pole gap, which

will be increased to 1.65 in for the new septum. Similarly, the C-magnet is a larger aperture (2.1 in instead of 1.6 in) and shorter (2.0 m instead of 3.0 m) version of the Main-Injector ICA magnet. An identical C-magnet is used in the extraction region. The descending beam in M3 will pass through the C-magnet first and will be bent upward by 38 mr. The beam will continue well above the center of the D3Q3 quadrupole and receive a 30-mr upward kick. Since the beam is up to 140 mm above the centerline of the quadrupole, a large-bore quadrupole magnet is required in order to provide adequate aperture. The large quadrupole at D3Q3 will be the LQE magnet from the D2Q5 location, which will be replaced by an 8-in quadrupole, as described below. The LQx magnets were designed to have a substantial good-field region that extends between the poles. Similar arrangements with LQ magnets can be found in Pbar at D4Q5 (former AP-2 injection, planned proton removal) and D6Q6 (former Debuncher extraction). The injected beam then passes through the field region of the septum magnet and receives a 37-mr upward bend as required for the necessary trajectory entering the injection kicker magnets. The kicker magnets provide a final 6.1-mr vertical bend to place the injected beam on the closed orbit of the Delivery Ring.

The two-module kicker system is located between the D30Q and D2Q2 magnets. To minimize the horizontal β function and maximize acceptance, the kickers will be located as close to the D2Q2 quadrupole as possible. Spare Pbar injection kicker magnets will be refurbished and reused for muon injection. The magnets are already designed to be oriented vertically, so little additional effort will be required to convert them to their new application. Kicker rise and fall time specifications and power supply information was provided in Table 4.8 and the accompanying text. Figure 4.29 shows the injection devices and their location in the Delivery Ring, along with their bend angles. Due to the large vertical excursion through the top of the D3Q2 magnet, a vertical bump across the injection region will be incorporated to lower the beam and improve the aperture. The quadrupole magnets at D2Q2, D30Q and D3Q4 will be displaced to create the bump by generating steering due to the beam passing off-center through the magnets. To create a 15-mm downward displacement at D3Q2, the magnets will be lowered by 8.1, 11.0, and 4.2 mm respectively. It would be beneficial, but not necessary for 40π -mm-mr acceptance, to install an existing “extended star chamber” quadrupole at the D3Q2 location. SQD-312, in magnet storage, was previously located at D4Q4 in the Pbar AP-2 injection area and has an extended top lobe in its star chamber.

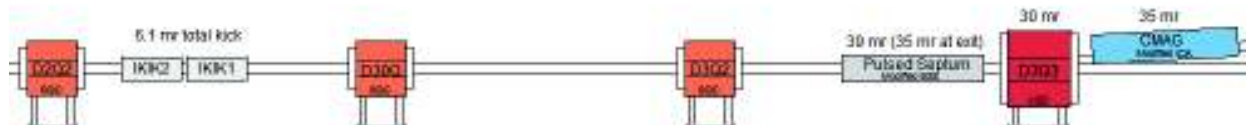


Figure 4.29: Delivery-Ring injection devices.

Extraction

Extraction from the Delivery Ring takes place in the downstream half of the 30 Straight Section. The extraction channel and the first 60 m of the M4 line will be used for both

Mu2e resonant extraction and $(g - 2)$ single-turn extraction. This arrangement avoids the complexity and additional expense of dual extraction lines in the limited available space. It also eliminates the need to remove potentially highly radioactive objects from the ring when switching between experiments. The ideal extraction configuration will provide enough aperture for both the Mu2e resonantly-extracted proton beam and the $(g - 2)$ muon beam to be transported efficiently through the M4 line.

A Lambertson and C-magnet pair will be used, in conjunction with the intervening D2Q5 quadrupole, to bend the beam upward out of the ring. In the interest of compatibility between $(g - 2)$, Mu2e, and future muon experiments, a Lambertson magnet is required for extraction. The resonant-extraction process used for Mu2e is very restrictive on the size, strength, and location of the electrostatic septa that are required to split the extracted beam. The electrostatic septa must be located on either side of the D2Q3 quadrupole, and are expected to be about 1.5 m in length. In order to achieve the goal of a combined extraction channel and beamline, the $(g - 2)$ extraction kickers must be located in a lattice location that is $n\pi/4$ radians from the Lambertson, where n is an integer, and in an area not already occupied by injection or extraction devices.

The $(g - 2)$ extraction kickers will be located between the D2Q2 and D2Q3 quadrupoles. There will be two kicker modules of approximately 0.85 m length each. During the dedicated period of $(g - 2)$ operation, the kickers will be located as close to the D2Q3 quadrupole as possible in order to minimize the vertical β function and maximize acceptance. The kicker magnets will be repurposed Pbar extraction kicker magnets that have a vertical aperture of 41 mm. The kicker magnets will be powered in series from a single power supply. There is also an alternative layout planned that would allow $(g - 2)$ to operate after the Mu2e electrostatic septa are installed. There is only room for a single kicker near the D2Q2 quadrupole in this arrangement, so the kicker inductance would need to be lowered to provide enough bending strength. The relocation of the kicker would also reduce aperture unless the β functions in this region could be suppressed by about 20%. Figure 4.30 shows the layout of the extraction devices for dedicated $(g - 2)$ operation and 40π -mm-mr acceptance.

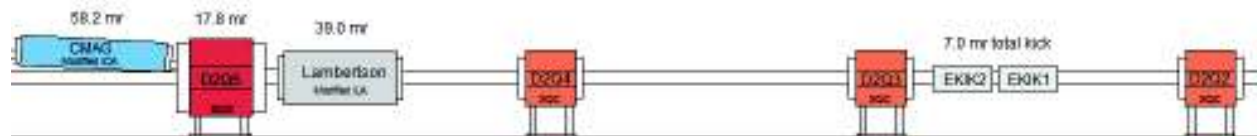


Figure 4.30: Delivery-Ring extraction devices.

Proton Removal (Abort) System

The proton removal system is an example of both repurposing an otherwise unneeded part of the Antiproton Source and implementing a dual function system that can be used by both $(g - 2)$ and Mu2e. During Mu2e operation, an abort is needed to minimize uncontrolled proton beam loss and to “clean up” beam left at the end of resonant extraction. The proton beam must be removed quickly, by means of kicker magnets, in order to minimize losses in

the ring. The $(g - 2)$ experiment can benefit from the removal of protons before they reach the storage ring. The abort system can serve this purpose, as long as the protons sufficiently slip in time to create a gap for the kickers to rise through.

The old Debuncher injection point from the AP-2 line in the D50 straight section will be used for the abort and proton removal systems. Recall that most of the AP-2 line will be removed and replaced with the new M2 line that will merge with the M3 line upstream of the right bend. The downstream end of AP-2, where antiprotons were formerly injected into the Debuncher, can now be used to extract protons from the Delivery Ring. This is made possible by the change in beam direction (as viewed from above) from clockwise to counterclockwise. The existing Pbar injection kicker magnets can be reused, although a new power supply will be needed to operate at the frequency needed to support Mu2e and $(g - 2)$. The septum magnet and power supply will also need to be upgraded for the same reason. The new larger-aperture septum magnet will be identical to what was previously described for injection into the Delivery Ring. The section of the AP-2 beamline being repurposed will require the addition of a vertical bending magnet to steer beam into the abort dump located in the middle of the Transport tunnel. Figure 4.31 shows the layout of the abort line.

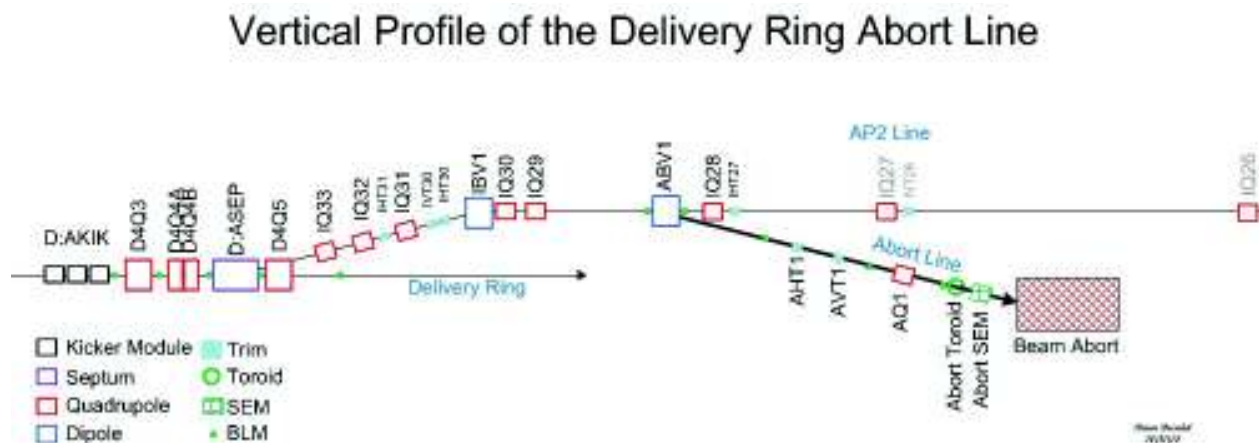


Figure 4.31: Side view of the Delivery Ring Abort/Proton Removal line.

The most economical plan is to power the three kicker magnets in series, which requires only a single power supply. The rise time of the kickers with this configuration is about 450 ns. This rise time is more than adequate for Mu2e operation, because the single 120-ns bunch is very short compared with the 8 GeV proton revolution period of 1695 ns. For $(g - 2)$ proton removal, the 450-ns rise time requires several revolutions around the Delivery Ring to provide enough gap between the muons and protons for the kicker to rise through. Table 4.9 lists the separation between the beams and the gap size for different numbers of turns. Seven turns around the Delivery Ring would be required to cleanly remove all of the protons without disturbing the muons. The table is based on the assumptions already stated: that the kicker rise time is 450 ns, the proton and muon bunch lengths are 120 ns and that the kicker should not disturb any of the muons.

As the kicker magnets “fill” during the rising current waveform, the kicker magnetic field and bending strength increase proportionally. Protons are completely removed from the Delivery Ring when the kicker strength is about 85% of what is needed to center beam

	Muon vs. Proton		Impact of proton removal kickers
	Centroid time difference (ns)	Gap size (ns)	
Injection	40	None	Unable to kick protons only
1 st turn at Abort	91	None	Unable to kick protons only
2 nd turn at Abort	161	41	11% of protons removed
3 rd turn at Abort	231	111	29% of protons removed
4 th turn at Abort	301	181	48% of protons removed
5 th turn at Abort	371	251	66% of protons removed
6 th turn at Abort	441	321	84% of protons removed
7 th turn at Abort	511	391	Protons cleanly removed
8 th turn at Abort	581	461	Protons cleanly removed

Table 4.9: Efficiency of proton-removal system for different number of turns in the Delivery Ring, based on a 120-ns bunch length and 450-ns kicker rise time.

in the abort channel. Between 85% and 100% of the nominal kicker strength, some of the protons will be lost on the Abort Septum instead of traveling to the abort. As the kicker strength drops below 85%, an increasing number of protons remain in the Delivery Ring.

In addition to separating the beams to improve removal efficiency, the percentage of protons removed can also be increased by firing the kicker earlier and disturbing part of the muons. Another option is to shorten the rise time of the kickers to 200 ns with the introduction of a second power supply and commensurate doubling of the power-supply cost. With a 200-ns kicker rise time, the gap between beams must be 168 ns or larger (achieved with 4 turns) to remove all of the protons.

A side benefit of the muons taking multiple turns around the Delivery Ring is that virtually all of the pions will have decayed before the muons reach the storage ring. The primary potential problem with this proton removal concept is due to differential decay systematic errors caused by the different muon path lengths as they travel through the Delivery Ring. Although a preliminary analysis indicates that this will not be a significant problem [17], a more thorough analysis is needed.

Vacuum Systems

The existing vacuum systems in the rings and transport lines have performed very well during Pbar operation. Typical vacuum readings in the Debuncher and transport lines were approximately 1×10^{-8} Torr. The Debuncher has good ion-pump coverage that should generally be adequate for $(g - 2)$ operation. Stochastic cooling tanks, kickers and septa that will be removed during the conversion have built-in ion pumps, so some of these pumps may need to be installed in the vacated spaces. Injection and extraction devices should have ion pumps integrated into the design, or there should also be additional pumping capacity added to the surrounding area. Vacuum components from the AP-2 and AP-3 lines should provide most of the needs for the reconfigured M2 and M3 lines. The Accumulator has enough surplus ion pumps and vacuum pipe available to cover part of the needs for the extraction beamlines.

Infrastructure Improvements

Electrical power for the Antiproton Source is provided by Feeder 24, which operated with a power level of about 4.4 MW during Pbar operation. Although the $(g - 2)$ power load is expected to be considerably less than what was used in Pbar by virtue of the reduced beam momentum, the Mu2e experiment must also be able to operate the same magnets at 8.89 GeV/c. For Mu2e, most service buildings are expected to use approximately the same amount of power as they did in Pbar operation. The exception is the AP-30 service building, where there will be a large increase in power load from the injection- and extraction-line power supplies. A new transformer may be needed at AP-30 to provide the additional power. A power test was performed on the individual service building transformers to aid in predicting the power needs for Mu2e [18]. Also, since the Accumulator will no longer be used, approximately 1.4 MW will be available for new loads.

Presently, Pbar magnets and power supplies receive their cooling water from the Pbar 95° Low Conductivity Water (LCW) system. The cooling requirements for $(g - 2)$ are expected to be lower than for Pbar operation. However, Mu2e will operate at 8.89 GeV/c and create a substantially larger heat load than $(g - 2)$. Fortunately, the removal of the heat load from decommissioning the Accumulator and the AP-2 line should be enough to offset the increase from the extraction line and other new loads. The extraction beamlines (M4 and $(g - 2)$ lines) will have an LCW stub line connecting to the Debuncher header in the 30 Straight Section. If necessary, it is also possible to design smaller closed-loop systems that heat-exchange with the Chilled Water system. The Chilled Water system has adequate capacity and is already distributed to the Pbar service buildings.

4.5.7 Muon transport to storage ring

4.6 Controls and beam monitoring

4.6.1 Accelerator controls

A well-established controls system allows devices in the former Antiproton-Source (“Pbar”), now Muon, service buildings and tunnel enclosures to receive information such as synchronization signals and to communicate back to other accelerator systems. A map of the service buildings, labeled “AP” for former Antiproton-Source buildings, and “F” for buildings which are part of the F-sector of the Tevatron, is shown in Fig. 4.32. Devices in the new extraction beamlines and MC-1 building will also need to be connected to the controls system.

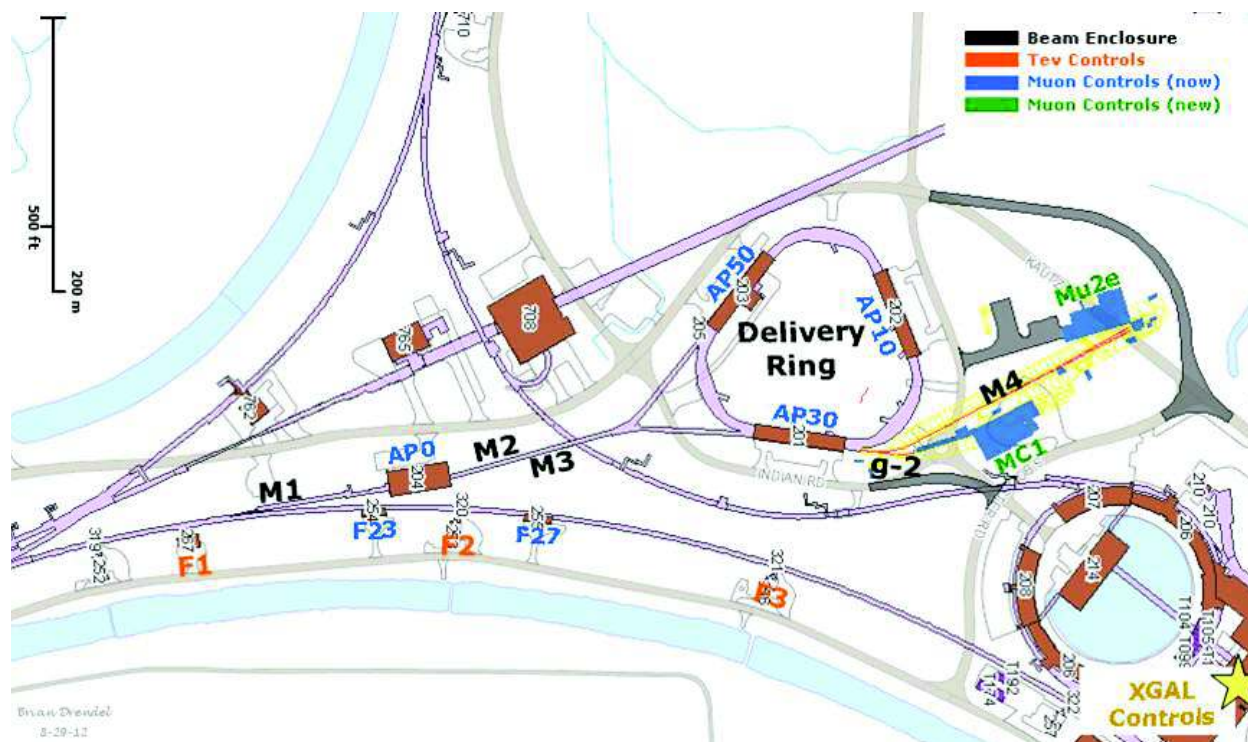


Figure 4.32: Muon Campus service buildings.

CAMAC and links

The existing accelerator service buildings will continue to use the legacy controls infrastructure that is currently in place. These service buildings include all of the Main Injector service buildings, as well as F0, F1, F2, F23, F27, AP0, AP10, AP30 and AP50. Future Muon Campus service buildings, including MC-1 and Mu2e, will be upgraded to a more modern controls infrastructure which will be discussed later in this document. Migration of the existing buildings to the more current controls standard is preferred and is being considered; however, sufficient funding is not available to start the upgrade path and it is believed that the existing infrastructure will be adequate for $(g - 2)$ operations.

Computer Automated Measurement and Control (CAMAC) crates exist in each service building and communicate with the control system through a VME-style front-end computer

over a 10 MHz serial link as shown in Fig. 4.33. Both digital and analog status and control of many accelerator devices occur through the CAMAC front ends. There should be no need to install additional CAMAC crates, as there is excess capacity in most of the existing crates. An inventory of existing CAMAC crates in the Muon service buildings shows that about 25% of the slots are unoccupied and could be used for additional CAMAC cards [19]. In addition, further slots have become available that were used to interface devices that became obsolete with the retirement of Collider Run II operations. It is anticipated that there will be ample CAMAC-crate coverage for $(g - 2)$ operation in the existing Muon service buildings, and very few crates will need to be added or moved.

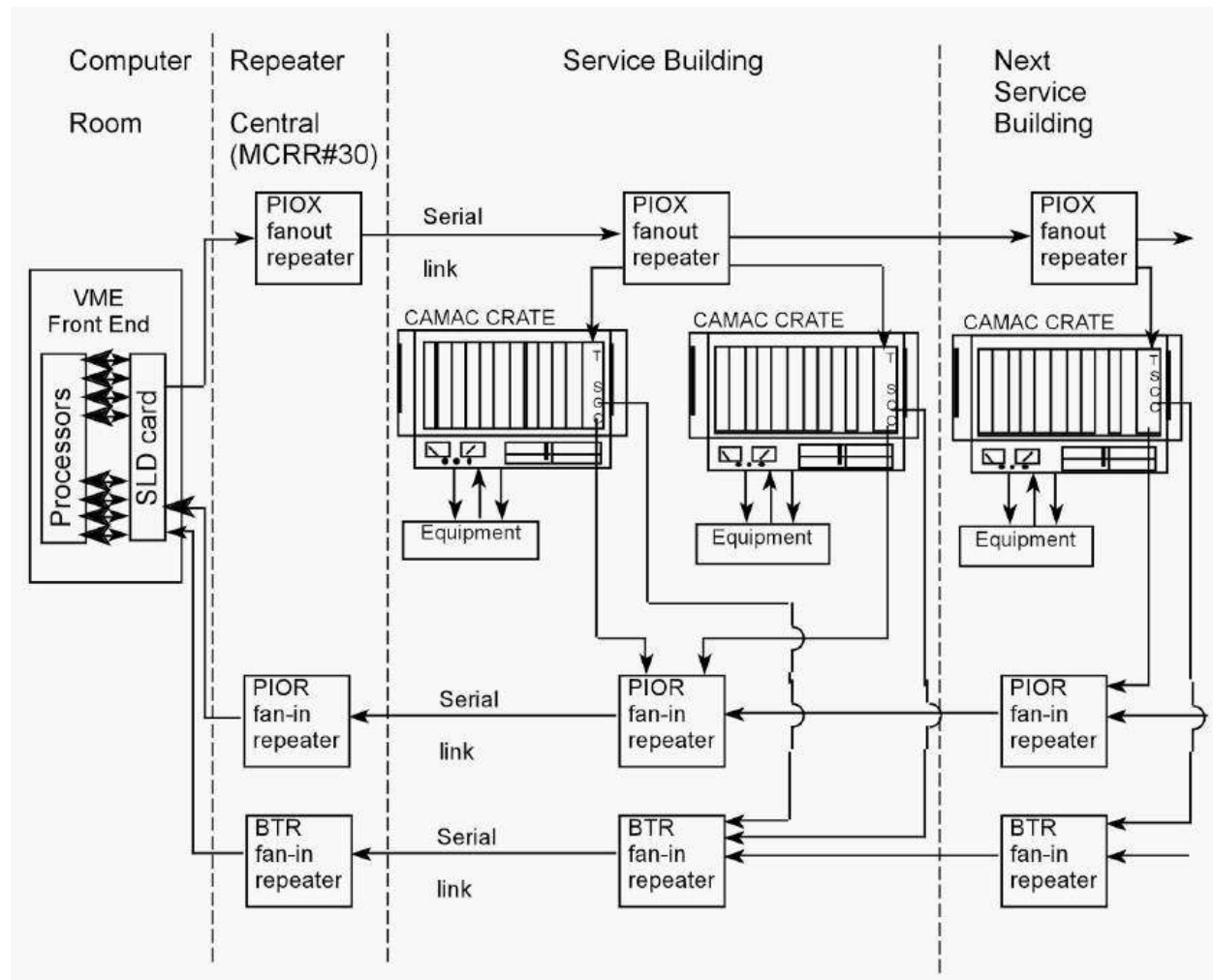


Figure 4.33: Legacy CAMAC crates interfacing VME front ends via serial links provide both analog and digital status and control of accelerator devices, and will continue to be used in existing Muon service buildings.

There are serial links that are distributed through and between the service buildings, via the accelerator enclosures, that provide the necessary communications paths for CAMAC as well as other necessary signals such as clock signals, the beam permit loop, and the Fire and Utilities System (FIRUS). Controls serial links can be run over multimode fiber-optic

cable or copper Heliac cable. Most Muon links that run through accelerator enclosures are run over Heliac, which should function normally in the radiation environment expected for $(g - 2)$ operations.

Accelerator device timing that does not require synchronization to the RF buckets will remain on the existing 10 MHz Tevatron Clock (TCLK) system. The existing TCLK infrastructure will remain in existing service buildings and new TCLK link feeds will be run via multimode fiber optic cable from the Mac Room to the new MC-1 and Mu2e service buildings.

Accelerator device timing for devices that require synchronization to the RF buckets will continue to be handled through the Beam Synch Clocks; however, a few changes will be required to maintain functionality. The F0, F1 and F2 service buildings will need both 53 MHz Main Injector beam synch (MIBS) for SY120 operations and 2.5 MHz Recycler beam synch (RRBS) for $(g - 2)$ and Mu2e operations. These buildings already support multiple beam synch clocks, so the addition of RRBS will require minimal effort. An obsolete 53 MHz Tevatron beam synch (TVBS) feed in the MI60 control room will be replaced with a 2.5 MHz RRBS feed in order to provide the necessary functionality. The remaining Muon service buildings currently use 53 MHz MIBS, but will require 2.5 MHz RRBS for $(g - 2)$ and Mu2e operations. This functionality can be obtained by replacing the MIBS feed at F0 with RRBS and using the existing infrastructure. Further upgrades and cable pulls will only be required if it is later determined that both MIBS and RRBS are required in these service buildings. New beam synch feeds to the $(g - 2)$ and Mu2e service building will be run via multimode fiber-optic cable from the Mac Room.

The Delivery-Ring permit loop provides a means of inhibiting incoming beam when there is a problem with the beam delivery system. The Pbar beam permit infrastructure will be used in the existing buildings. The CAMAC 201 and 479 cards, which provide the 50 MHz abort loop signal and monitor timing, will need to be moved from the Mac Room to AP50 to accommodate the addition of the abort kicker at AP50. Existing CAMAC 200 modules in each CAMAC crate can accommodate up to eight abort inputs each. If additional abort inputs are required, spare CAMAC 200 modules will be repurposed from the Tevatron and will only require an EPROM or PAL change. The permit loop will be extended to the MC-1 and Mu2e service buildings via multimode fiber-optic cable from the Mac Room. Abort inputs for these buildings will plug into a Hot-Link Rack Monitor abort card as will be mentioned below.

Operational and permit scenarios are under development. The capability of running beam to the Delivery-Ring dump when Mu2e and $(g - 2)$ are down will be needed, as well as the ability to run to either experiment while the other is down.

Hot-Link Rack Monitor

New controls installations will use Hot-Link Rack Monitors (HRMs) in place of CAMAC. A HRM runs on a VME platform that communicates with the control system over Ethernet as shown in Fig. 4.34. Unlike CAMAC, no external serial link is required, minimizing the need for cable pulls between buildings. Each HRM installation provides 64 analog input channels, 8 analog output channels, 8 TCLK timer channels, and 8 bytes of digital I/O. This incorporates the features of multiple CAMAC cards into a single, compact chassis.

Like CAMAC, when additional functionality or controls channels are needed, additional units can be added. As an example, a HRM version of the CAMAC 200 module will be constructed to provide inputs into the Delivery-Ring permit system. One or two HRMs will be installed in both the MC-1 and Mu2e buildings and should provide ample controls coverage for both accelerator and experimental devices.



Figure 4.34: A Hot-Link Rack Monitor is a flexible data acquisition system composed of a remote unit and a PCI Mezzanine card that resides in a VME crate. Each HRM provides sixty four 16 bit analog input channels, 8 analog output channels, 8 TCLK timer channels and 8 bytes of digital I/O. HRM.s will eventually replace all of the functionality of CAMAC [20].

HRMs are expected to eventually replace legacy CAMAC systems in the existing buildings. This migration will start by replacing existing 12-bit MADCs and CAMAC 190 cards for analog readings with 16-bit HRM channels. This option was considered for $(g - 2)$ operation, but was determined to be impractical considering expected funding, limited legacy Ethernet connectivity in three of the Muon service buildings, and the determination that the existing CAMAC would likely provide adequate performance for $(g - 2)$ operations.

Ethernet

Many modern devices have some form of Ethernet user-interface. In addition, many devices and remote front-ends use Ethernet to interface with the control system, instead of using the traditional CAMAC. The results are an increasing demand on the Controls Ethernet. Figure 4.35 is a map of the Muon Controls network. All of the current Muon Ring service buildings have Gigabit fiber-optic connections from the Cross-Gallery computer room to Cisco network switches centrally located in each service building. These will provide ample network bandwidth and connections after the reconfiguration for $(g - 2)$ and Mu2e. A central Ethernet switch that fans out to the other Muon Department buildings is currently located in AP10, but will need to be moved to AP30, as will be discussed later in this document.

Ethernet connects between the Muon-Ring service buildings via multimode fiber-optic cable paths that traverse the Rings enclosure on the Accumulator side. The multimode fiber currently in place will remain functional during $(g - 2)$ operations. However, in the higher-radiation environments expected during Mu2e operations, these fiber-optic cables will need

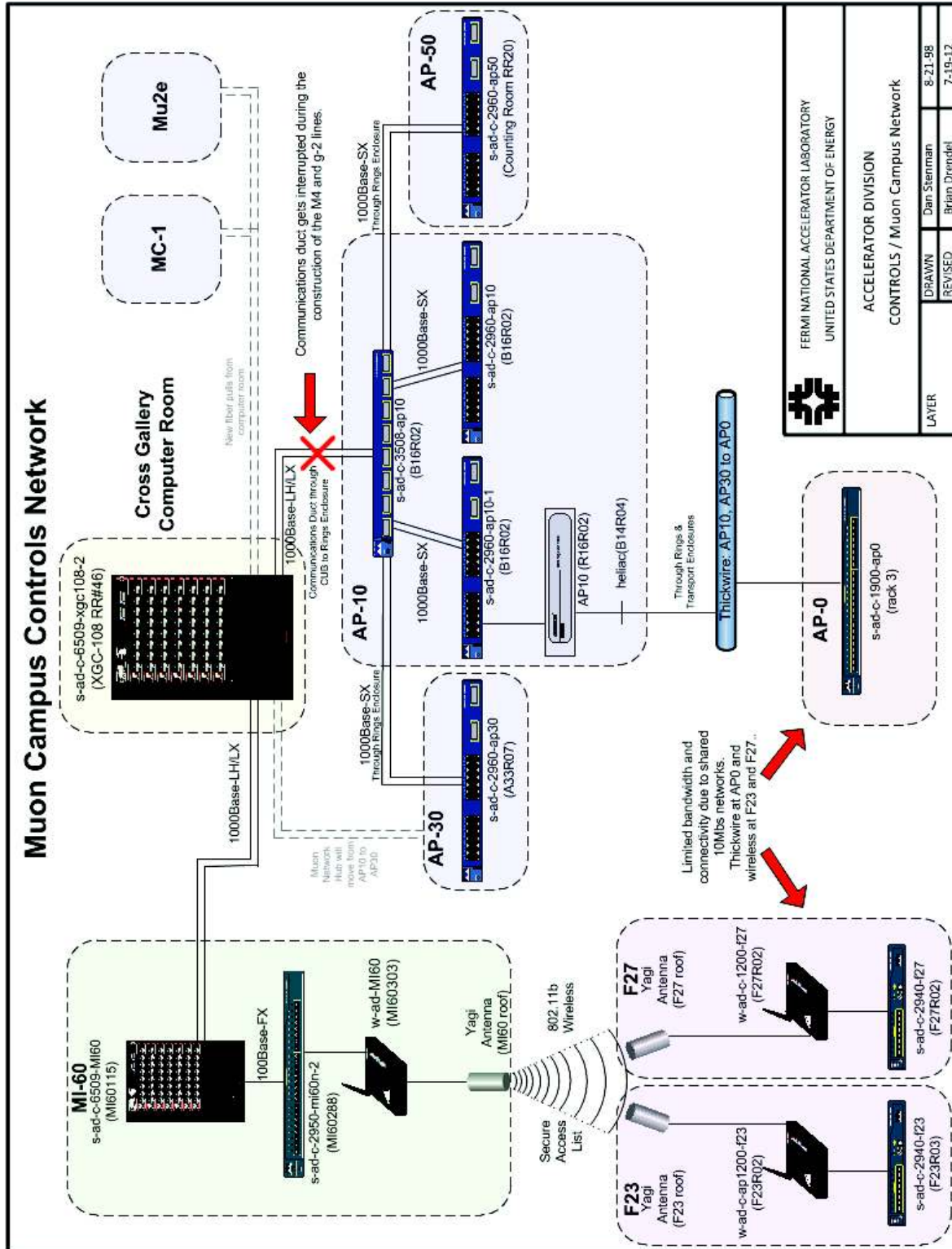


Figure 4.35: Controls Ethernet to the Muon Department service buildings is expected to be adequate for $(g - 2)$ operations. The central switch at AP10 will be moved to AP30. Legacy networks at AP0, F23, and F27 have limited bandwidth and connectivity.

to be upgraded to single-mode fiber at a minimum, or to the more costly radiation-hard fiber if radiation rates are too high.

Most beam line service buildings have gigabit fiber connected to centrally located network switches that provide ample network bandwidth and connections. AP0, F23, and F27 are the only three buildings that do not have this functionality. AP0 runs off a 10 Mbps hub that connects to 10Base5 “Thicknet” that runs through the Transport and Rings enclosures back to AP10, while F23 and F27 run off 802.11b wireless from MI60. Both are 10 Mbps shared networks with limited bandwidth and connectivity. It is anticipated that the network in these three buildings may be sufficient for $(g - 2)$ operations; however, network upgrade options are being considered, as will be discussed below.

Controls connectivity

Civil construction of the M4 and $(g - 2)$ beam line enclosures will result in the removal of the underground controls communication duct that provides the connectivity between the Accelerator Controls NETWORK (ACNET) and the Muon Campus [21]. Included in this communication duct is the fiber-optic cable that provides Ethernet connectivity, as well as 18 Heliac cables that provide the controls serial links and other signals including FIRUS. These cables currently connect from this communications duct to the center of the 20 location in the Rings enclosure, and travel through cable trays on the Delivery Ring side to the AP10 service building. After removal of the communications duct, FESS will construct new communications ducts from the existing manholes. These communications ducts will go directly to AP30, MC-1 and Mu2e service buildings without going through accelerator enclosures. See Fig. 4.36 for drawings of the current and future controls connectivity paths.

Restoring connectivity When the Heliac and fiber-optic cables are cut during the removal of the above-mentioned communications duct, controls connectivity will be lost. The base plan for restoring both Ethernet and controls-link connectivity is to pull new fiber optic cable from the cross gallery to the manhole outside of Booster Tower West and on to AP30 via the new communications duct. As a result of the new fiber pull, the Ethernet and controls links will fan out from AP30 instead of AP10. This will require some additional controls hardware configuration and labor. Efforts will be made to minimize the disruption by pulling the fiber and staging the new hardware at AP30 before the communication duct is cut. This is especially important for FIRUS which is necessary for monitoring building protection.

More details regarding the base plan and several alternatives, including cutting and splicing the Heliac cable or attempting to keep the fiber and Heliac intact during construction, can be found in Ref. [22].

Establish connectivity to MC-1 New fiber-optic cable will be pulled from the Mac Room to the MC-1 service building. Single-mode fiber is needed for Ethernet and FIRUS, and multimode fiber is needed for the timing links and the abort-permit loop. A single fiber bundle that contains 72 single-mode fibers and 24 multimode fibers will be pulled to MC-1. The fiber bundle will share a common path with the fiber bundles headed toward AP30 and Mu2e from the Cross Gallery to the manhole by Booster West Tower. All three fiber bundles



Figure 4.36: Muon campus controls paths. During construction of the M4 and $(g - 2)$ beamlines, the communications duct that provides controls connectivity to the Muon Campus will be interrupted. A new communications duct will be built to restore controls connectivity to the Muon service buildings. New controls will need to be established at the MC-1 and Mu2e buildings.

will travel through a single inner duct to the manhole. The Mu2e and MC-1 fiber bundles will then branch off to a second manhole inside a common inner duct, and then separate into the new communication ducts to the Mu2e and MC-1 service buildings. The fiber pulls will provide ample connectivity for all Ethernet and controls signals for both the accelerator and experiment. The $(g - 2)$ experiment anticipates requiring network rates approaching 100 MB/sec during production data taking which can be handled easily with the proposed infrastructure.

One alternate solution considered was to pull the new fiber along the existing communications duct until it intersected the extraction-lines enclosure. From there, the fiber could be directed along tunnel-enclosure cable trays to the MC-1 service buildings. Though this option would provide MC-1 cable-pull lengths of approximately the same length as the base option, it was eliminated due to the extra complications of pulling fiber through the tunnel enclosures to both Mu2e and AP-30. In both cases, the expected radiation environment would require a more expensive radiation-hard single-mode fiber. In addition, the CAMAC fiber links only run on multimode fiber, so link and clock repeaters would have to be re-designed to run on single-mode fiber, adding additional expense to the project.

Possible upgrades for legacy networks If the legacy Ethernet networks at AP0, F23, and F27 prove to provide insufficient connectivity or bandwidth for $(g - 2)$ operations, they can be most cost-effectively upgraded by replacing the current 10Base5 “Thicknet” with single-mode fiber-optic cable. The path would be from the AP30 service building to the

Rings enclosure, along the cable trays toward the M3 beam line, and down the Transport enclosure. From the Transport enclosure, the fiber-optic cable runs can go to F27 and AP0. An additional fiber-optic cable pull from AP0 through the PreVault enclosure provides a path to F23. The largest issue with this upgrade is that the single-mode fiber-optic cable is susceptible to radiation. If the radiation environment in the accelerator enclosures does not allow for single-mode fiber-optic cable, then radiation-hard fiber-optic cable can be pulled, but at a higher cost. Standard 96-count single-mode fiber costs approximately \$1.50/foot, whereas 96-count radiation-hard fiber costs approximately \$22/foot. Upgrading to the radiation-hard cable would add approximately \$50K to the cost of the cable pull. Other fiber-optic cable path options have been considered, but prove to be more costly to implement.

4.6.2 Accelerator instrumentation

Beam types

Beam monitoring can be divided into distinct zones: primary protons, mixed secondaries, proton secondaries, and muon “secondaries” (actually the dominant source of muons should be from the decay of the pion secondaries, so are technically “tertiary”). The locations of each of these areas are shown in Fig. 4.37. The expected beam properties in each of these areas are shown in Table 4.10.

Beam Type	Particle Species	Beam Momentum (GeV/c)	Number of Particles	RF Bucket (MHz)	Bunch Length (ns)	Transverse Emittance (mm-mrad)
Primary protons	p	8.9	10^{12}	2.515	120	18π
Mixed secondaries	μ^+ , π^+ , p, e^+	3.1	10^7 to 2×10^8	2.515	120	35π
Proton secondaries	p	3.1	10^7	2.515	120	35π
Muons	μ^+	3.1	$< 10^5$	2.515	120	35π

Table 4.10: Expected properties of primary proton beam, secondary beam off the target, and muon beam from pion decay relevant to instrumentation designed to measure beam. Transverse emittances are 95% normalized.

Primary proton beam Primary proton beam will traverse the Recycler, P1 stub, P1, P2 and M1 lines. Much of the instrumentation needed to measure the primary proton beam during ($g - 2$) operation already exists, but needs to be modified for use with the faster cycle times and 2.5 MHz RF beam structure. The overall beam intensity is similar to that seen in Pbar stacking operations, and in many cases requires only small calibration changes be made to the instrumentation. Toroids will be used to monitor beam intensity and will be used in conjunction with Beam Loss Monitors (BLMs) to maintain good transmission efficiency in the beamlines. Multiwires and Secondary Emission Monitors (SEMs) will provide beam profiles in both transverse planes. Beam Position Monitors (BPMs) will provide real-time orbit information and will be used by auto-steering software to maintain desired beam positions in the beamlines.

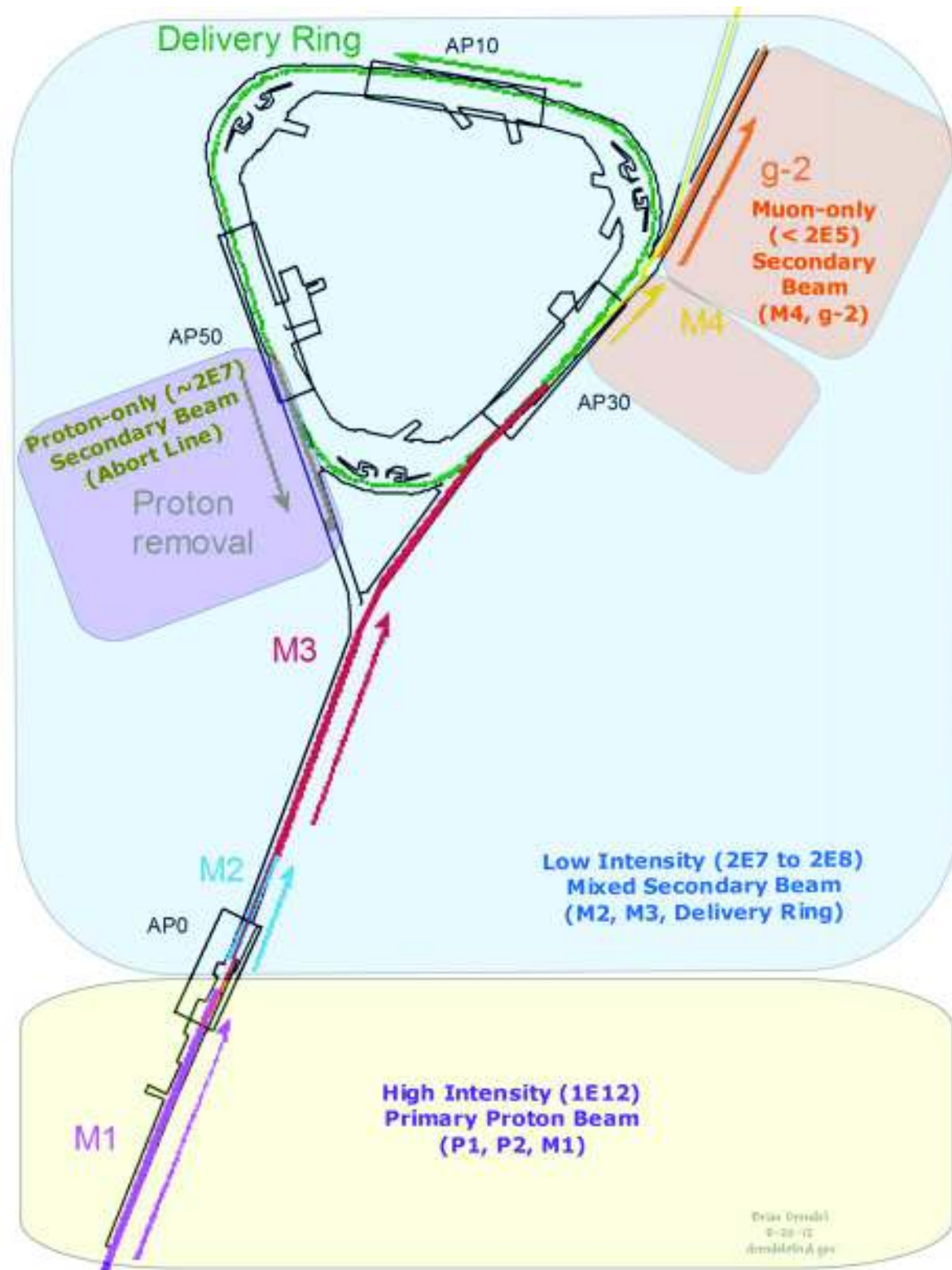


Figure 4.37: Beam monitoring can be divided into four different zones, each with different instrumentation schemes. High-intensity proton beam will be monitored with Toroids, BPMs and BLMs. Low-intensity secondary and proton-only secondary beam will be monitored with Ion Chambers, BPMs and SEMs. Muon-only secondary beam will be monitored with Ion Chambers and SWICs.

Toroids are beam transformers that produce a signal that is proportional to the beam intensity. There are two toroids in the P1 line, one in the P2 line and two in the M1 line. They will continue to be used in $(g - 2)$ operation to measure the primary proton beam. The electronics for these toroids are comprised of legacy analog processing inside of NIM crates. The base plan, due to funding limitations, is to continue to use the legacy electronics. If funding becomes available, the electronics would instead be upgraded to a VME-based processing environment, repurposing electronics from Collider Run II in order to provide cost savings. The existing toroids provide the majority of the required coverage, though the addition of a second toroid in the P2 line and a toroid in the P1 stub is desirable. The present toroid installation locations will be reviewed and modified as needed to provide adequate coverage. One possible change would be to move the upstream P1-line toroid downstream of the P1 line and P1 stub merge so that it could measure the beam injected into the P1 line from the stub. Filters, chokes, and preamps will be added for analog conditioning. Electronics will be modified, where necessary, to calibrate the toroids for $(g - 2)$ operations.

Beam line BPMs provide single-pass orbit-position information with sub-millimeter resolution, and will continue to be the primary beam-position devices in the P1, P2 and M1 lines. All BPMs share the Echotek style of electronics which was built as part of the Rapid Transfers Run II upgrade [23], and is the current standard for beam line BPMs. A functional diagram of the BPM hardware is shown in Fig. 4.38. These BPMs were designed to detect 7 to 84 consecutive 53 MHz proton bunches and four 2.5 MHz antiproton bunches for Collider Run II operations. Minimal electronics modifications will be required to measure the single 2.5 MHz bunches of 10^{12} particles expected during $(g - 2)$ operations. Two additional BPMs will be installed in the P1 stub.

Beam Loss Monitors are already in place in the P1, P2, and M1 beamlines. Existing ion-chamber detectors will be utilized for Mu2e operation. BLMs will be upgraded to modern BLM log monitor electronics, repurposing unused components from the Tevatron in order to minimize cost. An optional upgrade is being considered that would add snapshot capability to the BLMs. This feature would allow the loss monitors to distinguish losses from individual 15 Hz pulses of beam. However, this option adds significant cost to the BLM system. Two additional BLMs will be installed in the P1 stub.

There are two types of beam profile monitors in the beamlines: multiwires in the P1 and P2 lines, and SEMs in the other beamlines. The profile monitors will primarily be used for commissioning, studies, and documentation of the beamlines. General maintenance will be performed on the hardware and electronics to ensure proper functionality. The current location and wire spacing of the monitors will be reviewed and modified accordingly. Two additional multiwires will be installed in the P1 stub.

Mixed secondaries Mixed-secondary beam will traverse the M2 and M3 lines, as well as the Delivery Ring. Changes to existing instrumentation are required in these areas as a result of the secondary beam being approximately two orders of magnitude lower in intensity than that during the former Antiproton stacking operations. In addition, 2.515 MHz bunch structure and a faster pulse rate must be taken into consideration. Mu2e beam will have beam intensities four to five orders of magnitude higher than $(g - 2)$ operations in the M3 line and Delivery Ring, so design upgrades must take into account the vastly different

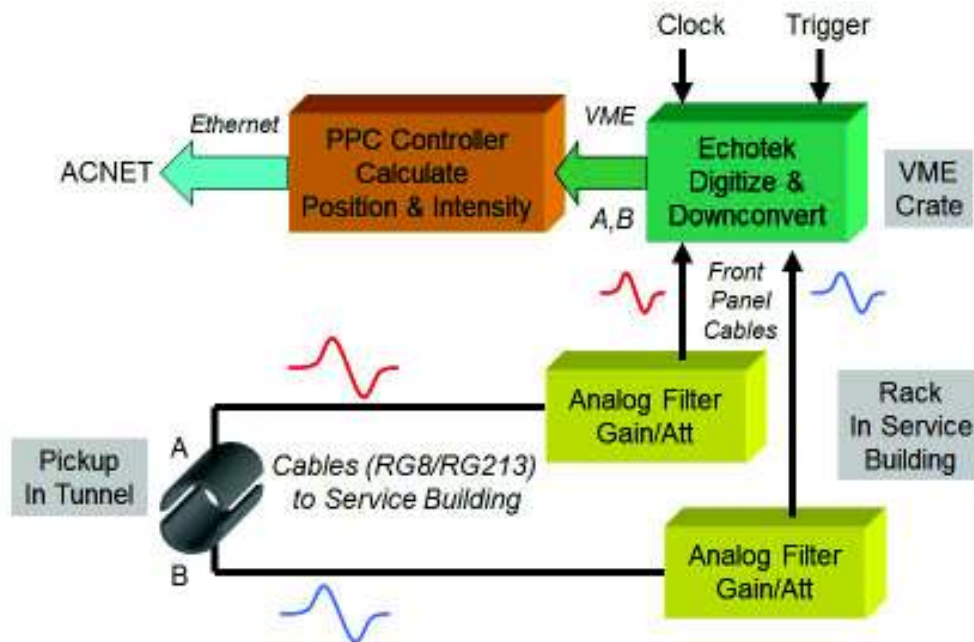


Figure 4.38: BPMs with Echotek processing electronics will be used to measure the transverse beam position of the 2.5MHz primary proton beam in the P1, P2 and M1 lines for $(g - 2)$ operations. The BPMs are not sensitive enough to see the low intensity secondary beams downstream of the AP0 target [23].

beam intensities required for both experiments. Beam studies have been conducted in order to help determine what instrumentation best suits the low-intensity secondaries of $(g - 2)$ operations [24].

Four toroids are available for use in the secondary beamlines and were the primary intensity-measurement device in these lines during Antiproton operations. These will be used for Mu2e operations; however, beam studies show that even with high gain and careful filtering, we were only able to measure beam intensities at levels one order of magnitude higher than $(g - 2)$ operational beam [24], as demonstrated in Fig. 4.39. As a result, toroids will likely not be used during normal $(g - 2)$ operations, but may still be used with higher-intensity beams during commissioning and studies periods.

A Direct-Current Current Transformer (DCCT) has been used in the Delivery Ring to measure beam intensity. This device will not function at $(g - 2)$ operational intensities and cycle time.

Ion chambers will become the primary beam-intensity measurement device for mixed-secondary beam. They are relatively inexpensive devices that can measure beam intensities with an accuracy of $\pm 5\%$ with as little as 10^5 particles. Ion chambers were used in the AP2 line in the past, and work was done during beam studies to recommission the ion chamber that used to be operational near the end of the AP2 line [24]. For $(g - 2)$ operations, one or two ion chambers will be implemented in the M2 line. Ion chambers are also being considered for the M3 line and the Delivery Ring; however, these would need to be installed in a vacuum can with motor controls to allow them to be pulled out of the beam during the

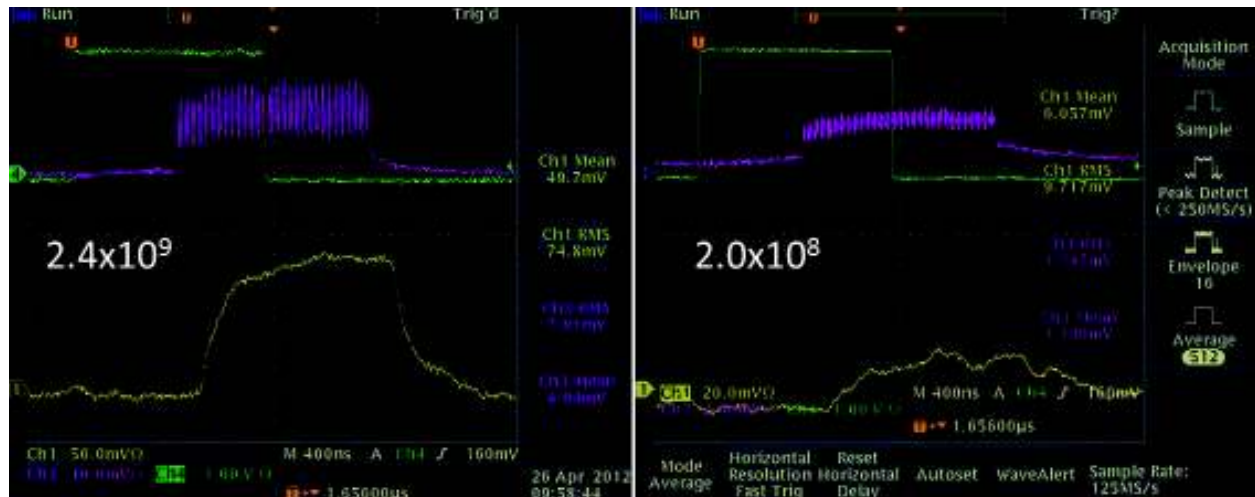


Figure 4.39: The yellow trace on both plots is a calibration test pulse on Toroid 724 in the AP2 line with high-gain preamps and special filtering to look for low-intensity beam. At beam intensities in the low 10^9 's, there is an easily-measurable beam signal. However, when the beam intensities are lowered to the level of 10^7 - 10^8 , the $(g - 2)$ expected secondary beam intensity range, beam intensities can not be measured.

higher-intensity Mu2e operations. Figure 4.40 shows an ion chamber installation in the AP2 line.

Wall Current Monitors (WCMs) are an alternative intensity-measurement device being considered for mixed-secondary beam. These devices have the advantage of being completely passive, and not requiring a break in the vacuum, which may make them a better fit in the M3 line where we need to stay compatible with the higher intensities of Mu2e operations, and the Delivery Ring where beam circulates for approximately 56 ms in Mu2e operations. New WCM designs are being considered that would provide accurate intensity measurements for secondary beam during $(g - 2)$ operations. The design is based on that of a WCM for Mu2e extraction. Each slice of the slow-spilled Mu2e beam is approximately 2×10^7 , which is consistent with the intensity that we would expect in the M3 line and Delivery Ring during $(g - 2)$ operations.

BPMs were a key diagnostic in Antiproton-Source operation providing sub-millimeter orbit information in the beamlines and Delivery Ring. BPMs are located at each quadrupole, providing ample coverage. There are 34 BPMs in the AP2 line, 28 BPMs in the AP3 line and 120 BPMs in the Delivery Ring; however, it is believed that the BPMs in these areas will not be able to see the low-intensity 2.515 MHz $(g - 2)$ secondary beam.

SEMs will be used to measure beam profiles in the M2 and M3 lines, as well as the Delivery Ring. There are eight SEMs in the AP2 line, seven SEMs in the AP3 line, three SEMs in the D/A line, two in the Debuncher, one in the Accumulator and three spares from the former AP4 line to draw from. SEM tunnel hardware will require some maintenance, and locations where SEMs are moved will require new cable pulls. Beam studies showed that special high-gain preamps will be required to measure the low-intensity secondary beam during $(g - 2)$ operations [24]. There are only two working high-gain preamps, so additional



Figure 4.40: Fixed-position ion chamber in the AP2 line. The ion chamber is separated from the beam pipe by a vacuum window on each side. Fixed-position ion chambers will only be used in the M2 line. In locations like the M3 line and Delivery Ring that will also see Mu2e beam, the ion chambers will be put inside of vacuum cans and made retractable.

preamps will need to be designed and fabricated. Additional SEMs will need to be added to the Delivery Ring from the pool of unused SEMs and spares. A photo of a SEM and its profile display are shown in Fig. 4.41.

BLMs (Fig. 4.42) will be used to help maintain good transmission efficiency through the lines. Both Delivery-Ring and AP3 loss monitors will use the existing hardware and electronics for $(g-2)$ operations, but will be replaced for the higher-intensity Mu2e operations. Care will need to be taken to make a BLM plan that allows for switching back and forth between the two separate BLM systems.

Proton Secondaries Proton secondaries will be extracted to the Delivery Ring abort line and will have a similar beam intensity to that of the Delivery Ring. Existing instrumentation from the downstream AP2 line will be used. A toroid will be used to measure beam intensity for Mu2e operations, but will be out of its operational range for $(g-2)$. If intensity measurement is needed, a retractable ion chamber will be added to the line. Ion chambers, SEMs and BLMs will be used in the same way they are for the mixed secondary lines.

Muon Secondaries Muon secondaries will traverse the upstream portion of the M4 line and the $(g-2)$ line. The largest technical challenge will be measuring muon secondary beam, which models show should be on the order of 10^5 muons per pulse. This is two or three orders of magnitude smaller than the upstream mixed-secondary beam. Most diagnostics will not work at these beam intensities.

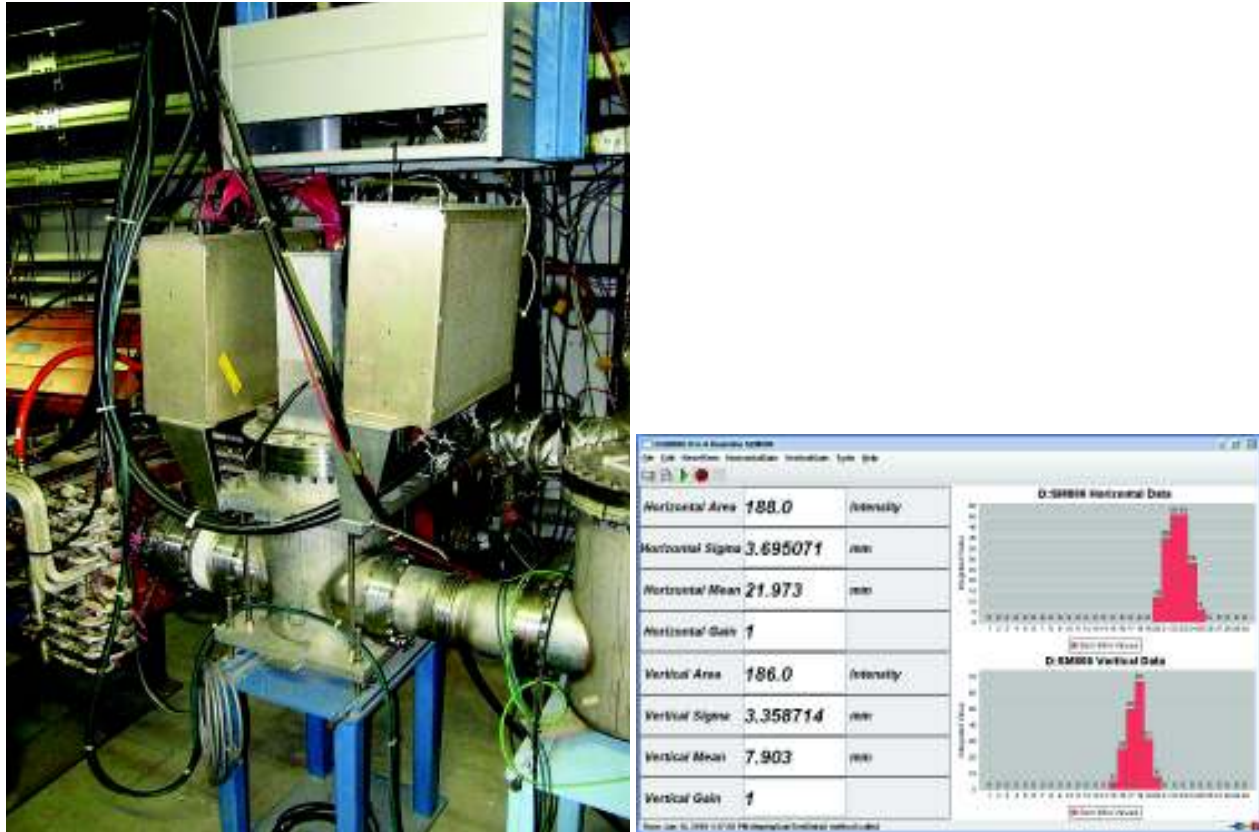


Figure 4.41: SEMs will be used to measure mixed secondary beam profiles. SEM tunnel hardware (left) is pictured. Preamp boxes are mounted next to the vacuum can. The SEM wires can be pulled out of the beam when not in use. SEMs can be used with to measure beam profiles, positions and intensities (right).

Beam intensity will be measured with ion chambers that are designed with three signal foils and four bias foils to increase the signal amplification. This design will allow beam intensity measurements down to 10^5 particles. The ion chamber in the M4 line will need to be retractable in order to be compatible with Mu2e operations, while the $(g - 2)$ -line ion chambers can be permanently in the beam path. New ion chambers will be designed and built because there is not a pool of available spares to populate these beamlines. A Wall Current Monitor is another option being considered for beam-intensity measurement in the upstream M4 line. Though this device may be able to measure the Mu2e slow-spill beam intensity, it is not clear if one could be designed that is sensitive enough to see the lower-intensity muon beam expected for $(g - 2)$ operations.

Three options have been considered for measuring beam profiles. The base plan uses Segmented Wire Ion Chambers (SWICs), which are very similar to Multiwires with the exception that the beam goes through ArCO_2 gas, which is ionized by the charged-particle beams, creating an amplification that allows measurements of beam intensities down to the 10^4 particle range. This is an order of magnitude lower than the expected $(g - 2)$ operational beam. In addition, SWICs are robust enough to handle particle beams several orders of magnitude higher in intensity than are expected during $(g - 2)$ operations. This

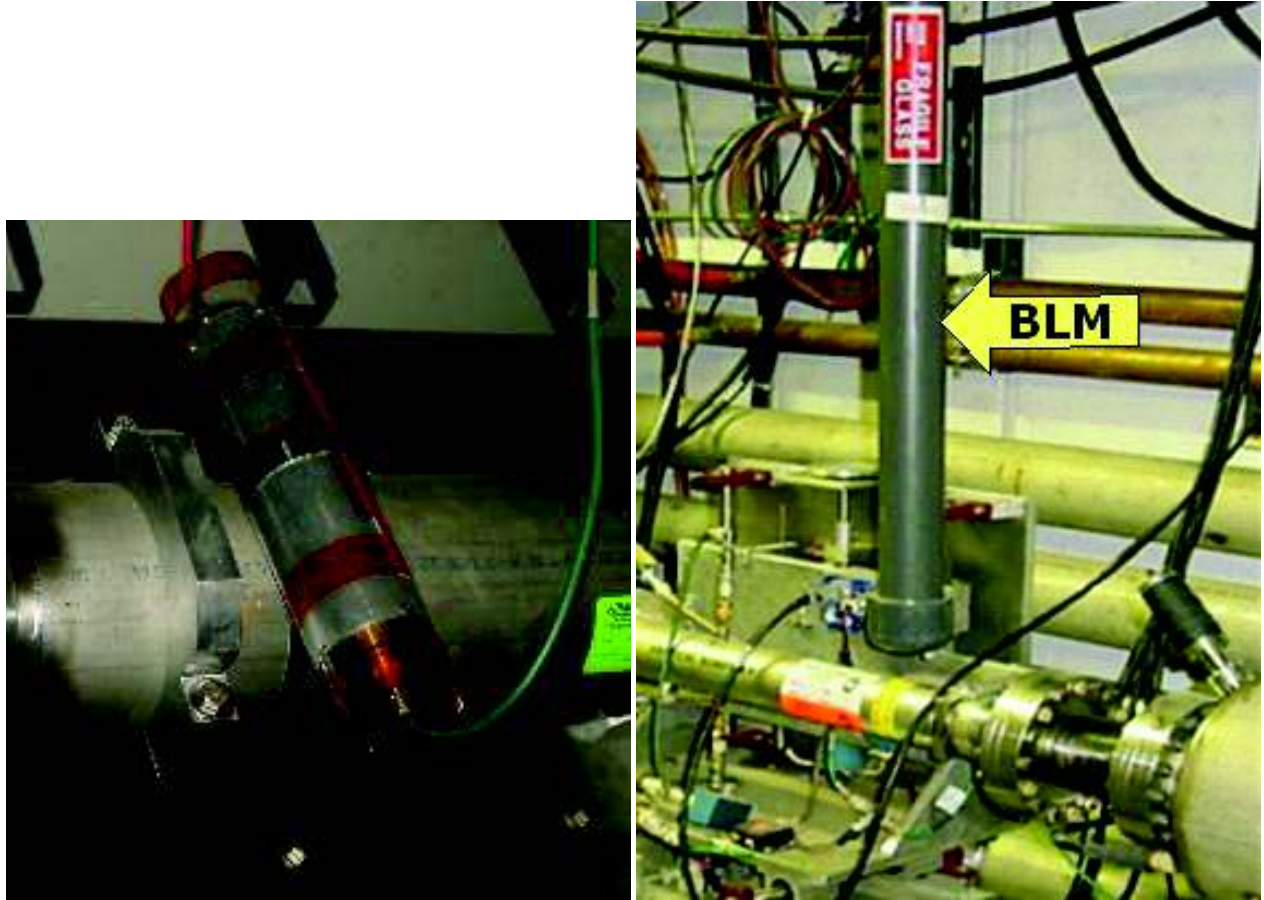


Figure 4.42: Two styles of BLMs will be used. Tevatron-style ion chamber loss monitors (left) will be used in areas of primary beam, and also in the Delivery Ring for Mu2e operations. The Pbar-style ion chamber, which consists of a plastic scintillator and a long light guide connected to a photomultiplier tube shielded from light in PVC, will be used in the Delivery Ring during ($g - 2$) operations.

will provide the flexibility of running higher-intensity protons through the M4 and $g - 2$ lines for commissioning and beam studies. The SWICs will need to be retractable since they are a destructive measurement device. Some vacuum cans can be acquired from other systems to minimize the cost; however, the inventory of spare vacuum cans is not sufficient enough to cover all of the SWICs.

A second option that was considered is the Proportional Wire Chamber (PWC). The advantage of the PWC is that it can measure beam down to 10^3 particles, and the wire planes are modular. The major disadvantage is that the wires are easily damaged by higher-intensity pulses, limiting the ability to run higher intensity study beam.

The third option that was considered is to design Scintillator Fiber Profile Monitors (SFPs), which can measure down to 100 particles. These devices are similar to SWICs or PWCs, but the wires are replaced with scintillating fiber. They have been used in the SY120 test-beam lines, and the fibers have been shown to survive long periods of beam operation. The largest disadvantage is that SFPs cost significantly more than SWICs.

The upstream M4 line will be made compatible with both Mu2e and $(g - 2)$ operations. Beam in the M4 line for $(g - 2)$ will be at least two orders of magnitude smaller than the individual slices of slow-spilled beam that the line will see in Mu2e operations.

Intensity and profile information will also need to be collected just before and after the inflector, which will likely be achieved with ion chambers and some combination of the profile-measurement devices mentioned above. The two primary factors limiting the instrumentation after the inflector are a much smaller available physical space and potentially lower-intensity beam.

If muon beam profile information cannot be accurately measured with the proposed diagnostics, one option being considered is to develop a tune-up mode. In this mode, protons in the Delivery Ring would not be sent to the abort, but extracted toward $(g - 2)$ with the muon beam. This would result in 10^7 particles per pulse in the extraction lines, which is easily measured by ion chambers and SWICs.

Accelerator instrumentation summary

A summary of instrumentation devices which will potentially be used for $(g - 2)$ is shown in Table 4.11.

Beamline	Beam type	Intensity	Position	Profile	Loss
Primary protons	P1, P2, M1	toroids	BPMs	multiwires, SEMs	BLMs
Mixed secondaries	M2, M3, DR	ion chambers, WCMs	SEMs	SEMs	BLMs
Proton secondaries	DR abort	ion chambers, WCMs	SEMs	SEMs	BLMs
Muons	M4, $(g - 2)$	ion chambers, WCMs	SWICs, PWCs, SFPMs		

Table 4.11: Potential instrumentation to be used in the beamlines for $(g - 2)$ operations.

4.7 Radiation Safety Plan

4.8 ES&H, Quality Assurance, Value Management

References

- [1] W. Pellico *et al.*, “Proton Source Task Force Report”, Beams Doc. 3660 (2010); F. G. Garcia *et al.*, “Fermilab Proton Improvement Plan Design Handbook”, Beams Doc 4053 (2012).
- [2] D.S. Ayres *et al.*, “NO ν A Technical Design Report”, NO ν A Doc 2678 (2007).
- [3] D. Still *et al.*, “ $g - 2$ Yield Beam Study Results – April 2012”, $g - 2$ Doc 430 (2012).
- [4] I. Kourbanis, “Bunch Formation for $g - 2$ experiment”, $g - 2$ Doc 335 (2012).
- [5] M. Xiao, “Transport from the Recycler Ring to the Antiproton Source Beamlines”, Beams Doc 4085 (2012).
- [6] N. Mokhov, <http://www-ap.fnal.gov/MARS>.
- [7] C. Yoshikawa *et al.*, “Optimization of the Target Subsystem for the New $g - 2$ Experiment”, IPAC2012.
- [8] S. Striganov, “Optimization of $g - 2$ Target Parameters”, Fermilab Doc GM2-doc-197.
- [9] Muons, Inc., <http://www.muonsinc.com/muons3/G4beamline>.
- [10] B. Drendel *et al.*, “Antiproton Source Rookie Book”, Beams-doc-2872, June 2010.
- [11] ANSYS®, <http://www.ansys.com>.
- [12] R. Shultz, “ANSYS Mechanical Simulation for Lithium Lens”, Fermilab Doc GM2-doc-362.
- [13] C. Hojvat *et al.*, “The Fermilab Tevatron I Project Target Station For Antiproton Production”, Fermilab TM-1175 (March 1983).
- [14] D.C. Carey, K.L. Brown, F. Rothacker, FERMILAB-Pub-98/310 (1998).
- [15] $g - 2$ Doc 484 (2012).
- [16] V. Lebedev, $g - 2$ Doc 171 (2012).
- [17] $g - 2$ Doc 252 (2012).
- [18] J.P. Morgan, “Power tests for Pbar service buildings”, Mu2e Doc 2117 (2012).

- [19] B. Drendel *et al.*, “Pbar Controls Reference Material”, Mu2e-doc-1161, May 2012.
- [20] A. R. Franck *et al.*, “HOTLink Rack Monitor”, FERMILAB-Conf-01/342/E.
- [21] B. Drendel *et al.*, “Controls to Mu2e/g-2/Muon and Communications Duct Issues”, Mu2e-doc-2069, February, 2012.
- [22] communications duct details and alternative plans
- [23] N. Eddy and E. Harms, “Beamline BPM Upgrade”, Beams-doc-1279, September 2004.
- [24] D. Still *et al.*, “ $g - 2$ Yield Beam Tests”, G2M-doc-430, July 2012.